RESEARCH REPORT

HEALTH EFFECTS INSTITUTE

Number 136
January 2009

PRESS VERSION

Uptake and Inflammatory Effects of Nanoparticles in a Human Vascular Endothelial Cell Line

Ian M. Kennedy, Dennis Wilson, and Abdul I. Barakat

Uptake and Inflammatory Effects of Nanoparticles in a Human Vascular Endothelial Cell Line

Ian M. Kennedy, Dennis Wilson, and Abdul I. Barakat

with a Critique by the HEI Health Review Committee

Research Report 136
Health Effects Institute
Boston, Massachusetts

Trusted Science • Cleaner Air • Better Health

Publishing history: The Web version of this document was posted at *www.healtheffects.org* in January 2009 and then finalized for print.

Citation for whole document:

Kennedy IM, Wilson D, Barakat AI. 2009. Uptake and Inflammatory Effects of Nanoparticles in a Human Vascular Endothelial Cell Line. HEI Research Report 136, Health Effects Institute, Boston, MA.

When specifying a section of this report, cite it as a chapter of the whole document.

 Asterisk Typographics, Barre, Vt., Compositor. Printed by Recycled Paper Printing, Boston, Mass. Library of Congress Catalog Number for the HEI Report Series: WA 754 R432.

Cover paper: made with at least 50% recycled content, of which at least 15% is post-consumer waste; free of acid and elemental chlorine. Text paper: made with 100% post-consumer recycled product, acid free; no chlorine used in processing. The book is printed with soy-based inks and is of permanent archival quality.

CONTENTS

Research Report 136

ABOUT HEI

The Health Effects Institute is a nonprofit corporation chartered in 1980 as an independent research organization to provide high-quality, impartial, and relevant science on the effects of air pollution on health. To accomplish its mission, the institute

- Identifies the highest-priority areas for health effects research;
- Competitively funds and oversees research projects;
- Provides intensive independent review of HEI-supported studies and related research;
- Integrates HEI's research results with those of other institutions into broader evaluations; and
- Communicates the results of HEI research and analyses to public and private decision makers.

HEI receives half of its core funds from the U.S. Environmental Protection Agency and half from the worldwide motor vehicle industry. Frequently, other public and private organizations in the United States and around the world also support major projects or certain research programs. HEI has funded more than 280 research projects in North America, Europe, Asia, and Latin America, the results of which have informed decisions regarding carbon monoxide, air toxics, nitrogen oxides, diesel exhaust, ozone, particulate matter, and other pollutants. These results have appeared in the peer-reviewed literature and in more than 200 comprehensive reports published by HEI.

HEI's independent Board of Directors consists of leaders in science and policy who are committed to fostering the public–private partnership that is central to the organization. The Health Research Committee solicits input from HEI sponsors and other stakeholders and works with scientific staff to develop a Five-Year Strategic Plan, select research projects for funding, and oversee their conduct. The Health Review Committee, which has no role in selecting or overseeing studies, works with staff to evaluate and interpret the results of funded studies and related research.

All project results and accompanying comments by the Health Review Committee are widely disseminated through HEI's Web site (*www.healtheffects.org*), printed reports, newsletters, and other publications, annual conferences, and presentations to legislative bodies and public agencies.

ABOUT THIS REPORT

Research Report 136, *Uptake and Inflammatory Effects of Nanoparticles in a Human Vascular Endothelial Cell Line*, presents a research project funded by the Health Effects Institute and conducted by Ian Kennedy of the University of California–Davis and his colleagues. This report contains three main sections.

The HEI Statement, prepared by staff at HEI, is a brief, nontechnical summary of the study and its findings; it also briefly describes the Health Review Committee's comments on the study.

The Investigators' Report, prepared by Kennedy et al., describes the scientific background, aims, methods, results, and conclusions of the study.

The Critique is prepared by members of the Health Review Committee with the assistance of HEI staff; it places the study in a broader scientific context, points out its strengths and limitations, and discusses remaining uncertainties and implications of the study's findings for public health and future research.

This report has gone through HEI's rigorous review process. When an HEI-funded study is completed, the investigators submit a draft final report presenting the background and results of the study. This draft report is first examined by outside technical reviewers and a biostatistician. The report and the reviewers' comments are then evaluated by members of the Health Review Committee, an independent panel of distinguished scientists who have no involvement in selecting or overseeing HEI studies. During the review process, the investigators have an opportunity to exchange comments with the Review Committee and, as necessary, to revise their report. The Critique reflects the information provided in the final version of the report.

HEI STATEMENT

Synopsis of Research Report 136

Uptake and Inflammatory Effects of Nanoparticles in a Human Vascular Endothelial Cell Line

BACKGROUND

Epidemiologic and toxicologic studies indicate that ambient particulate matter (PM)—a complex mixture of solid and liquid particles suspended in air—has multiple effects on health. One of the key issues in assessing the health effects of PM is determining the physical characteristics (such as size and charge) and chemical characteristics most responsible for toxicity. Particles ≤ 10 μm in aerodynamic diameter (PM_{10}) are of most concern because these particles are respirable by humans. To protect the general population and groups considered most vulnerable to adverse effects from PM in the United States, the Environmental Protection Agency monitors PM_{10} levels and has promulgated National Ambient Air Quality Standards for particles ≤ 2.5 μm in aerodynamic diameter ($PM_{2.5}$, or fine particles). Some scientists believe that particles < 100 nm in diameter may be particularly toxic. These particles are referred to as ultrafine (< 100 nm in all dimensions) or nanoparticles (with at least one dimension < 100 nm). Several studies have suggested that metals may be important toxic components of the PM mixture.

A further key issue is the identification of pathways by which particles interact with cells in the airways and other cells to exert toxic effects. Some studies suggest that after inhalation small particles move rapidly out of the lung, enter the bloodstream, and affect other tissues. Because endothelial cells—a layer of specialized cells that line the interior of blood vessels—serve as a barrier between tissues and the bloodstream, the passage of inhaled particles from lungs into the circulation and then into tissue implies that particles have the opportunity to interact with the endothelial layer. Because responses of endothelial cells also play a critical role in the development of atherosclerosis, and because exposure to particles has been reported to affect the development of atherosclerosis, understanding the response of endothelial cells to particles may be important.

In response to HEI's Request for Preliminary Applications RFPA 04-6, Dr. Ian Kennedy and colleagues at the University of California–Davis, proposed to generate nanoparticles of the oxides of four different metals—iron, zinc, yttrium, and cerium. They chose these metals because iron and zinc are abundant in urban and diesel exhaust PM, iron and cerium are components of recently developed automobile technologies, and yttrium can be "tagged" with a fluorescent marker to identify the localization of particles taken up into cells. The investigators also proposed to evaluate the size and composition of the particles, and to study their potential to induce inflammatory effects in human aortic endothelial cells (HAECs). The investigators also proposed to identify where inside the HAECs the particles would be found after co-culture with the cells. The investigators hypothesized that the biologic effects of the particles would differ depending on their chemical composition and physical properties. The Health Research Committee recommended the study for one year of funding, to determine whether the proposed approaches would be successful.

APPROACH

Dr. Kennedy and colleagues used a flame combustion system to generate nanoparticles of the oxides of iron, zinc, yttrium, and cerium. They characterized several physical properties of the particles, using inductively coupled plasma–mass spectrometry, X-ray diffraction, transmission electron microscopy (TEM), and a scanning mobility particle sizer. They also calculated the particles' surface area.

This Statement, prepared by the Health Effects Institute, summarizes a research project funded by HEI and conducted by Dr. Ian Kennedy and colleagues at the University of California–Davis. Research Report 136 contains both the detailed Investigators' Report and a Critique on the study prepared by the Institute's Health Review Committee.

The investigators incubated particles in solution in a range of concentrations with an HAEC line in vitro, for 4 hours in most experiments. The HAECs were evaluated for the induction of reactive oxygen species (ROS) and markers of oxidative stress and inflammation. Because their attempt to use a fluorescent tagging approach to identify particles within HAECs was not successful, the investigators used TEM on HAECs to identify the subcellular localization of the particles. Responses to cerium oxide particles were evaluated in only a few experiments.

RESULTS AND INTERPRETATIONS

The nanoparticles generated varied in morphology (spherical, cubic, or rod-shaped), agglomeration, and size range (from spherical particles of iron oxide [in two ranges—less than 5 nm in diameter and 30–90 nm diameter] to rod-shaped zinc oxide particles 100–200 nm long). The metal oxides showed a range of effects on HAECs. Of the particles tested, zinc oxide was associated with the greatest number of effects (increasing levels of some markers of inflammation and one measure each of ROS generation and oxidative stress); zinc oxide particles also affected the adherence of HAECs to the substrate and may have resulted in death of the HAECs that became nonadherent. Yttrium oxide was associated with changes in a few end points—specifically, increases in markers of inflammation and one measure of ROS generation. Iron oxide and cerium oxide had no biologic effects on any of the end points measured. The investigators calculated the surface areas of the different particles and found them to be in the following order: iron oxide (larger size range) > yttrium oxide > zinc oxide and cerium oxide.

Zinc, yttrium, and iron oxide particles were detected within HAECs (cerium oxide was not evaluated). The appearance and localization of the three metal oxides differed within the cells.

CONCLUSIONS

Kennedy and colleagues generated iron, zinc, yttrium, and cerium oxide nanoparticles and identified some of their important physical characteristics: size and shape, agglomeration, and calculated surface area. These properties differed for each type of particle. Preliminary studies to characterize effects of the different particles on inflammatory end points and the generation of ROS and oxidative stress in HAECs showed that the different metal oxide particles induced different patterns of biologic responses. Zinc oxide affected more end points than yttrium oxide, whereas iron oxide and cerium oxide had no effects.

The Health Review Committee, which independently reviewed the study, agreed with the investigators' general conclusions about the biologic responses induced by the different particles: namely, that the effects induced by co-culture of HAECs with nanoparticles depended on the composition of the particles. However, the Committee thought that the differences in biologic responses may have resulted from differences among the particles not only in the physical properties the investigators reported, but also in other, unexamined physical properties, such as solubility and surface charge. Thus, the Committee thought that the investigators had developed a potentially useful model system with HAECs, but that the study's results would have been strengthened if some of these other particle characteristics had been further explored.

The investigators interpreted the findings to indicate that biologic activity was inversely correlated with surface area. The HEI Review Committee agreed that particle surface area is likely to be one important factor in determining biologic effects, but the Committee was not convinced by the investigators' interpretation because cerium oxide had the same surface area as zinc oxide but had no biologic effect.

Kennedy and colleagues showed that the particles were taken up by HAECs, with some evidence that the particles may have localized to different compartments in the cell. The Review Committee did not think this evidence was clear-cut, however, and was not convinced that the reported biologic effects were related to differential localization of the particles within HAECs.

Extrapolating the current study's findings to in vivo human responses is challenging. The physiological relevance of the responses of endothelial cells in vitro to the concentrations of metal particles used in the current study is uncertain. However, occupational exposure to high concentrations of inhaled metal particles has been associated with adverse respiratory and systemic inflammatory and cardiovascular effects. Thus, characterizing the physical and chemical properties of well-defined metal oxide nanoparticles and the effects they induce in vivo and in vitro merits further study.

INVESTIGATORS' REPORT

Uptake and Inflammatory Effects of Nanoparticles in a Human Vascular Endothelial Cell Line

Ian M. Kennedy, Dennis Wilson, and Abdul I. Barakat

ABSTRACT

The mechanisms governing the correlation between exposure to nanoparticles and the increased incidence of cardiovascular disease remain unknown. Nanoparticles appear to cross the pulmonary epithelial barrier into the bloodstream, raising the possibility of direct contact with the vascular endothelium. Because endothelial inflammation is critical for the development of cardiovascular pathology, we hypothesized that direct exposure of human aortic endothelial cells (HAECs*) to nanoparticles induces an inflammatory response and that this response depends on the composition of the particles. To test this hypothesis, we incubated HAECs for 1 to 8 hours with different concentrations (0.001–50 μg/mL) of iron oxide (Fe_2O_3), yttrium oxide (Y_2O_3), cerium oxide (CeO_2), and zinc oxide (ZnO) nanoparticles. Using real-time reverse transcriptase–polymerase chain reaction (RT–PCR), we subsequently measured messenger RNA (mRNA) levels of three markers of inflammation: intercellular cell adhesion molecule-1 (ICAM-1), interleukin-8 (IL-8), and monocyte chemotactic protein-1 (MCP-1). The particles were well characterized in terms of size, surface area, composition, and crystal structure. To determine the interactions of nanoparticles with HAECs, we used inductively coupled plasma–mass spectrometry (ICP–MS) to measure the concentration of internalized particles. Our data indicate that the delivery of nanoparticles to the HAEC surface and their uptake within the cells correlate directly with the concentration of particles in the cell culture medium. Transmission electron microscopy (TEM) revealed that the Fe_2O_3, Y_2O_3, and ZnO nanoparticles are internalized by HAECs and are often found within intracellular vesicles (the CeO_2 particles were not imaged). Fe_2O_3 nanoparticles did not provoke an inflammatory response in HAECs at any of the concentrations tested, CeO_2 particles elicited no response at low concentrations and a weak response above 10 μg/mL, and Y_2O_3 and ZnO nanoparticles elicited a pronounced inflammatory response above a threshold concentration of 10 μg/mL. We used fluorescent markers to identify the production of reactive oxygen species (ROS) in cells; the results showed that Y_2O_3 and ZnO particles at the highest concentrations may lead to the production of ROS. At the highest concentration, ZnO nanoparticles caused significant loss of cell adherence. These results demonstrate that inflammation in HAECs after acute exposure to metal oxide nanoparticles depends on the concentration and composition of the particles.

INTRODUCTION

Although recent epidemiologic studies have demonstrated a correlation between exposure to fine particulate matter in air pollution and increased cardiovascular morbidity and mortality (Samet et al. 2000; Peters et al. 2001; Pope et al. 2004), the mechanisms behind this correlation remain largely unknown. In other studies, nanoparticles (100 nm or smaller) have been reported to be particularly relevant pathologically because of their small size, which allows them to be transported deep into the lung, and high degree of reactivity. Of particular relevance to the present study, nanoparticles have been shown to cross the pulmonary epithelial barrier into the bloodstream (Kreyling et al. 2002; Nemmar et al. 2002, 2003); the result is that the vascular endothelium, the monolayer of cells lining the inner surfaces of blood vessels, is directly exposed to particles.

* A list of abbreviations and other terms appears at the end of the Investigators' Report.

This Investigators' Report is one part of Health Effects Institute Research Report 136, which also includes a Commentary by the Health Review Committee and an HEI Statement about the research project. Correspondence concerning the Investigators' Report may be addressed to Dr. Ian M. Kennedy, Department of Mechanical and Aeronautical Engineering, University of California, One Shields Ave. Davis, CA 95616; *imkennedy@ucdavis.edu*.

Although this document was produced with partial funding by the United States Environmental Protection Agency under Assistance Award CR–83234701 to the Health Effects Institute, it has not been subjected to the Agency's peer and administrative review and therefore may not necessarily reflect the views of the Agency, and no official endorsement by it should be inferred. The contents of this document also have not been reviewed by private party institutions, including those that support the Health Effects Institute; therefore, it may not reflect the views or policies of these parties, and no endorsement by them should be inferred.

Atherosclerosis is a primary cause of many cardiovascular complications, including myocardial infarction, ischemia, and stroke. Acute and chronic inflammation of the endothelium plays a central role in the development of atherosclerosis (Ross 1999; Libby 2002). We hypothesized that exposure of HAECs to nanoparticles of metal oxide would elicit a rapid inflammatory response and that the nature of the response would depend on the composition of the particles. To test this hypothesis, we exposed cultured HAECs to nanoparticles of Fe_2O_3, Y_2O_3, ZnO, and CeO_2 at a wide range of concentrations for periods of 1 to 8 hours and subsequently assessed the impact of these exposures on mRNA and protein levels of specific inflammatory markers. We also used various imaging and spectrometric techniques to probe the interactions of particles with cells. We chose the four metals because of their environmental relevance and use in technology, including engine technology.

SPECIFIC AIMS

In this one-year preliminary study, we proposed to work with cultured HAECs as a model for the effects of exposure to nanoparticles of metals on cardiovascular health. We chose to explore the impact of particle composition on the uptake of the particles, the production of ROS, and the inflammatory response to the particles. We intended to work with four metals that span a range of expected reactivities within cellular vesicles: cerium, yttrium, iron, and zinc. In addition to examining the responses of the cells to these particles, we intended to make use of nanoparticles with phosphor materials (europium-doped Y_2O_3 particles ($Eu:Y_2O_3$), for example) that can be imaged within cells and examined with confocal microscopy for colocalization with labeled structures, thus allowing us to positively identify the vesicles that sequester particles.

MATERIALS AND METHODS

SYNTHESIS OF METAL OXIDE NANOPARTICLES

Fe_2O_3 nanoparticles were synthesized in an H_2/air diffusion flame seeded with the vapor of $Fe(CO)_5$ (iron pentacarbonyl) (99.5%, Alfa Aesar, Ward Hill, MA) using the system described by Guo and Kennedy (2004). The $Fe(CO)_5$ vapor decomposed in the flame to form Fe_2O_3 nanoparticles. This compound, which sublimed at moderately high temperature, was placed in a stainless steel basket in a furnace and produced a vapor upon heating. ZnO nanoparticles were similarly synthesized in an H_2/air diffusion flame seeded with the vapor of the metal zinc. Zinc shots, millimeter-sized spheres of zinc metal (99.999%, Alfa Aesar), were placed in a stainless steel basket in a furnace that was heated to approximately 600°C. The post-flame aerosol containing the particles was drawn into a sampling tube by vacuum, and the particles were captured on a membrane filter. Y_2O_3 nanoparticles were synthesized in the same manner with the vapor of tris(2,2,6,6-tetramethyl-3,5-heptanedionate)Y(III) (98%, Alfa Aesar).

The synthesis of CeO_2 posed problems, since there is no suitable high-vapor-pressure precursor of CeO_2. Therefore, we needed to use a soluble solid precursor to deliver cerium to a flame. Figure 1 shows a schematic diagram of the spray flame burner used to synthesize CeO_2 particles. It was used in a closed chamber with ventilation to prevent possible exposure of laboratory personnel. The precursor solution of 30-mM cerium acetate in deionized water was nebulized at a rate of 0.333 mL/min by a flow of air at 2.0 L/min. The aerosol of 10-to-20-μm droplets was entrained by a hydrogen flow of 1.8 L/min and fed to a coannular nozzle. Either 2.0 L/min of oxygen or 2.0 L/min of nitrogen was used in the co-flow to vary the flame temperature slightly. A cold finger, a cooled surface that attracts particles by the process of thermophoresis, was used to collect particles; samples were scraped off the surface of the cold finger after collection. They were washed using 100% ethanol and sonicated in a bath for 30 minutes to break up loose aggregates generated during sample collection. Finally, they were dried and stored.

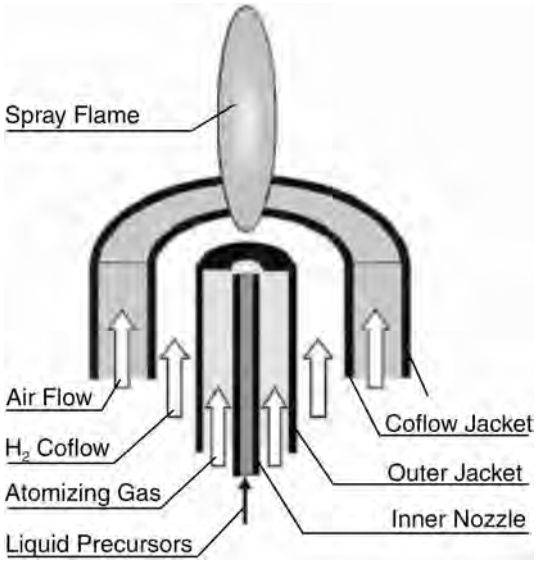

Figure 1. Schematic diagram of spray flame burner.

Synthesis of Eu:Y_2O_3 Particles

Spray pyrolysis was used to synthesize Eu:Y_2O_3 particles. Soluble nitrate precursors of europium and yttrium were dissolved in water, nebulized into a spray, and introduced to an H_2/air diffusion flame. The oxide nanoparticles were collected on a cold finger. The europium ion emits light at 612 nm when excited with ultraviolet radiation at 260 nm. It was therefore used as a luminescent label in following the translocation of nanoparticles.

CHARACTERIZATION OF NANOPARTICLES

Fe_2O_3, Y_2O_3, and ZnO nanoparticles were characterized using TEM. All four particle types were characterized using x-ray diffraction (XRD) and the Brunauer-Emmett-Teller (BET) technique for surface-area measurement. For the TEM and XRD analyses, the nanoparticles (except for the CeO_2 particles, which were collected on the cold finger) were first extracted from the membrane filter and suspended in ethanol. To prepare an XRD sample, the ethanol suspension containing the metal oxide particles was deposited dropwise on a single crystal silicon substrate and dried to obtain a thin layer of the particles. The XRD samples were then analyzed in a Scintag PAD V x-ray diffractometer with a Cu K_α radiation source operated at 45 kV and 40 mA. The XRD patterns were analyzed using the MDI JADE 6.0 program. To prepare samples for TEM, drops of the ethanol suspension were put on copper TEM grids with carbon film support. After the solvent had evaporated, at room temperature, the metal oxide nanoparticles were deposited on the grids. The TEM samples were then analyzed using a Philips CM-12 microscope operated at 100 kV. To measure the size distributions of the Fe_2O_3 and CeO_2 particles in situ, we used a TSI scanning mobility particle sizer (SMPS), consisting of a 3071A differential mobility analyzer and a 3025A condensation particle counter (CPC) (TSI Inc., Shoreview, MN). A sampling probe was constructed with a 1.3-cm-diameter stainless steel tube, which was placed at a height of 6 cm above the tip of the flame. By taking samples at a sufficiently large distance from the flame and thus diluting the aerosol with the surrounding air, we could avoid overloading the CPC.

The BET analysis was conducted using a Gemini 2360 instrument (Micromeritics, Norcross, GA). Each sample contained 50 to 100 mg nanoparticles. To remove adsorbed water, samples were first degassed at 300°C to reach a pressure lower than 10 µm Hg; the water content was determined gravimetrically. The specific surface area of the nanoparticle samples was then measured by N_2 adsorption or desorption.

We also determined the detailed metal composition of iron, yttrium, and zinc particles using ICP–MS. The results demonstrated that the particles were pure—concentrations of the vast majority of trace metals were below the detection limit for all three types of nanoparticles. In the few cases where trace metal impurities were detected, they were at concentrations on the order of 0.01 ppb (very close to the detection limit [data not shown]).

CELL CULTURE AND EXPOSURE TO NANOPARTICLES

Standard procedures were used to culture HAECs (Cascade Biologics, Portland, OR) in passages 5 to 8 in Medium 200 (Cascade Biologics) containing 100 U/mL penicillin G, 100 µg/mL streptomycin, 0.25 µg/mL amphotericin B, and Low Serum Growth Supplement (LSGS) (Cascade Biologics). The addition of LSGS resulted in a medium containing 2% fetal bovine serum, 1 µg/mL hydrocortisone, 10 ng/mL human epidermal growth factor, 3 ng/mL basic fibroblast growth factor, and 10 µg/mL heparin.

For cell culture experiments, dry nanoparticles were resuspended in endotoxin-free distilled water, and the stock solution was kept under sterile conditions at 4°C for use in individual experiments. The concentration of all four nanoparticle stock solutions was the same (7.3 mg/mL). Before they were diluted and added to cell cultures, nanoparticle stock solutions were sonicated for 5 minutes to break up aggregates.

Confluent HAEC monolayers in standard 6-well plates were incubated for 1 to 8 hours at 37°C with Fe_2O_3, Y_2O_3, or ZnO nanoparticles in cell culture medium at concentrations ranging from 0.001 to 50 µg/mL. CeO_2 particles were incubated with HAECs for 4 hours only, owing to limited time and resources. The results, however, are useful in determining the differential potential of a range of relevant metal oxides for initiating inflammation in HAECs. HAECs incubated in nanoparticle-free medium served as controls.

To determine the effects of nanoparticles on the viability of HAECs, cells that were incubated with the ZnO, Y_2O_3, and Fe_2O_3 nanoparticles for 4 hours were washed twice with complete phosphate-buffered saline (PBS) (Invitrogen, Carlsbad, CA) and then subjected to the trypan blue exclusion assay. To assess both shorter- and longer-term effects of nanoparticle exposure on HAEC viability, the trypan blue assay was performed immediately after the 4-hour incubation period, as well as 24 hours after the end of incubation (during which time the cells were incubated in nanoparticle-free cell culture medium).

ISOLATION OF RNA AND REVERSE TRANSCRIPTION

Immediately after incubation with nanoparticles, HAECs were washed with PBS, detached by trypsinization, and collected by centrifugation. Total RNA was isolated using

phenol and guanidine isothiocyanate (TRIzol Reagent; Invitrogen) and chloroform in accordance with the manufacturer's instructions. To isolate the RNA, whole-cell lysate in the TRIzol reagent was mixed with chloroform. Cell proteins and DNA were extracted into the organic phase, and whole-cell RNA was left in the aqueous phase after centrifugation of the solution. The RNA was subsequently precipitated with isopropanol, and the final cell pellet was resuspended in DEPC-treated water (Ambion, Austin, TX) and stored at −80°C. Complementary DNA (cDNA) was prepared from 1 μg of total RNA using a reverse transcriptase enzyme (SuperScript II, Invitrogen) according to the manufacturer's instructions.

QUANTITATIVE REAL-TIME PCR ANALYSIS

Levels of transcription of three inflammatory markers—ICAM-1, MCP-1, and IL-8—were determined. Human glyceraldehyde-3-phosphate dehydrogenase (GAPDH) was used as an internal control. Primers for these markers were designed by Primer Express (Applied Biosystems, Foster City, CA) and purchased from Operon Technologies (Alameda, CA). Their sequences were as follows:

ICAM-1 sense: 5′-CAGAAGAAGTGGCCCTCCATAG-3′

ICAM-1 antisense: 5′-GGGCCTTTGTGTTTTGATGCTA-3′

MCP-1 sense: 5′-GCCAAGGAGATCTGTGCTGAC-3′

MCP-1 antisense: 5′-CATGGAATCCTGAACCCACTTC-3′

IL-8 sense: 5′-GTGTAAACATGACTTCCAAGCTGG-3′

IL-8 antisense: 5′-GCACCTTCACACAGAGCTGC-3′

GAPDH sense: 5′-CACCAACTGCTTAGCACCCC-3′

GAPDH antisense: 5′-TGGTCATGAGTCCTTCCACG-3′

Quantitative real-time PCR was conducted using the GeneAmp 7900HT Sequence Detection System (Applied Biosystems). The reaction was performed in MicroAmp optical 96-well reaction plates (Applied Biosystems) with 25 μL of reaction mixture in each well. The reaction mixture contained samples of cDNA diluted 1:10, 500 nM of the respective sense and antisense primers, and SYBR Green PCR Master Mix (Applied Biosystems). Control samples were diluted at 1:10, 1:20, 1:40, 1:80, and 1:160 to create standards for a standard curve. The PCR reaction consisted of initial thermal activation of the mixture at 95°C for 10 minutes (40 cycles). Each cycle was as follows: 95°C for 15 seconds and 60°C for 1 minute.

PCR products were verified by analysis of heat-dissociation curves and amplification plots. Quantitative values were acquired from linear regression of the PCR standard curve, and levels of expression of gene markers of inflammation were normalized to GAPDH levels for each sample. Experiments were run in duplicate and repeated three times for each of the four types of nanoparticle.

WESTERN BLOT ANALYSIS

Immediately after incubation with nanoparticles, HAECs were washed with PBS and then lysed using a lysis buffer containing M-PER Mammalian Protein Extraction reagent (Pierce, Rockford, IL), sodium orthovanadate, sodium fluoride, phenyl methyl sulfonyl fluoride, protease inhibitor cocktail (containing 4-(2-aminoethyl)benzenesulfonyl fluoride, pepstatin A, E-64, bestatin, leupeptin, and aprotinin) (Sigma, St. Louis, MO), and Triton X-100. Electrophoresis of protein solutions was performed on a 7.5% Tris-HCl gel (Bio-Rad Laboratories, Hercules, CA) for 45 minutes at 150 V. Proteins were then transferred onto a nitrocellulose membrane. The membrane was blotted and incubated overnight at 4°C with rabbit polyclonal anti–ICAM-1 (Santa Cruz Biotechnology, Santa Cruz, CA) and mouse monoclonal anti–β-actin (Sigma, St. Louis, MO) as primary antibodies, followed by incubation with horseradish peroxidase (HRP) conjugated anti-rabbit and anti-mouse secondary antibodies. HRP was visualized using ECL Western Blotting Detection Reagent (Amersham, Pittsburgh, PA) and developed on a film (Pierce). Protein analysis was performed using Kodak 1D Image Analysis Software (Kodak, Rochester, NY). Band densities of ICAM-1 were normalized by the band density of β-actin, which served as an internal control.

ENZYME-LINKED IMMUNOSORBENT ASSAY ANALYSIS

Immediately after the period of incubation with nanoparticles, cell culture supernatants were collected and centrifuged at 14,000 rpm for 5 minutes to remove cell debris and particles. Concentrations of MCP-1 protein in the supernatants were assayed using an enzyme-linked immunosorbent assay (ELISA) kit (Quantikine human CCL2/MCP-1 Immunoassay; R&D Systems, Minneapolis, MN) according to the manufacturer's instructions. The supernatants of as few as two experiments and as many as four were tested; each sample was run in duplicate.

TEM OF CELLS

HAECs exposed to nanoparticles for 4 hours were washed with PBS and fixed with Karnovsky electron microscopy fixative (2.5% glutaraldehyde and 2% paraformaldehyde in 80 mM phosphate buffer at pH 7.3-7.4). Secondary fixation was performed in 1% osmium tetroxide with 1.5% potassium ferrocyanide in double-distilled H_2O for 1 hour at 4°C. Dehydration was achieved through the use of

ascending concentrations of ethanol, with three changes at 100%. Pure Epon-Araldite resin that did not contain nadic methyl anhydride was added and infiltrated overnight at room temperature. All excess resin was removed the next day, and fresh resin was added to the appropriate depth. The sample was polymerized for 18 hours. Ultrathin sections of cells of interest were cut en face (parallel to the surface on which the cells were grown) using a Leica Ultracut UCT ultramicrotome (Leica Mikrosysteme GmbH, Austria) and then stained with uranyl acetate and lead citrate before being viewed in a Philips CM-12 electron microscope.

ICP–MS

The delivery of the metal oxide nanoparticles to the cell surface and the uptake of the nanoparticles by the cells were measured using ICP–MS. Confluent HAECs in 6-well plates were exposed for 4 hours to nanoparticles, washed with PBS, and detached by trypsinization. Each cell pellet was resuspended in 0.5-mL Hanks balanced salt solution (HBSS) (Invitrogen), and the number of cells was determined using a hemacytometer (Bright-Line; Hausser Scientific, Horsham, PA). The solutions were mixed with concentrated nitric acid (HNO_3) (EMD Chemicals, Gibbstown, NJ), to reach a final HNO_3 concentration of 3%, and then heated to 80°C for 3 hours to dissolve the cell content. A blank control solution (without cells) was prepared for ICP–MS analysis by mixing 0.5 mL of HBSS with the same amount of concentrated HNO_3; the mixture was then processed in the same way as the sample solutions. Finally, the solutions were adjusted to a volume of 25 mL with 3% HNO_3 in water. The concentrations of iron, yttrium, and zinc in the solutions were determined using an Agilent Technologies 7500c ICP–MS. The precision of the analysis was better than ± 3.8%. Cerium was not analyzed using ICP–MS.

DETECTION OF INTRACELLULAR OXIDATION

We used several approaches to detect intracellular ROS production. The first was to use the dye CM-H_2DCFDA (5-[and-6]-chloromethyl-2′,7′-dichlorodihydrofluorescein diacetate, acetyl ester) (Invitrogen), which fluoresces when oxidized. Pretreatment of cells with CM-H2DCFDA followed by a treatment that generates ROS initiates fluorescence that can be detected either by fluorescence microscopy or by a fluorescence plate reader (Liu, 2001). We preloaded HAECs grown on fibronectin-coated coverslips with 1 µM/mL CM-H_2DCFDA in Krebs-Henseleit buffer in the dark for 45 minutes. Cells were washed with PBS and incubated with test particulate preparations for 2 and 4 hours.

Then we exposed endothelial cell monolayers grown on glass coverslips to laboratory-generated particles of Fe_2O_3, ZnO, and Y_2O_3 at concentrations of 1 and 10 µg/mL. To compare the responses of laboratory-generated particulate matter (PM) with more environmentally relevant particles, we similarly treated cell monolayers with 1 and 10 µg/mL of National Institute of Standards and Technology (NIST) standard urban particles. To control for potential redox activity of soluble iron, we incubated monolayers with 1 and 10 mg/mL of Fe_2O_3 in solution. As a maximum positive control for the ROS assay, we incubated cultures with 1% H_2O_2 (hydrogen peroxide).

Cells were then rinsed in PBS and fixed for 10 minutes in 1% paraformaldehyde. Digital images of six randomly chosen high-power fields were obtained with an Olympus Provis fluorescent microscopy system. Quantitation of fluorescence was done by first converting images to gray-scale with Photoshop (Adobe Systems) and then determining the total fluorescent density (the summation of the total gray values, in pixels, for the region imaged) using the integrated density-analysis tool of ImageJ image-analysis software.

As an alternative, additional approach to evaluating ROS generation, we repeated the above experiment that evaluated ROS production using CM-H_2DCFDA and particles of Fe_2O_3, ZnO, and Y_2O_3, this time with translocation of Nrf2 to the nucleus as an end point. Nrf2 is a transcription factor involved in the activation of antioxidant response genes. Under baseline conditions, Nrf2 is sequestered in the cytoplasm by Keap1, a cysteine-rich regulator protein. Oxidation of the sulfhydryl-containing residues on Keap1 as a result of electrophiles, including ROS, causes Nrf2 to dissociate from Keap1 and translocate to the nucleus. Using an immunofluorescent antibody probe for Nrf2, we counted positively stained nuclei in endothelial cell cultures treated in a manner similar to that used in the CM-H_2DCFDA experiments.

Another approach we took to detect intracellular oxidative activity was to use dihydroethidium (DHE) (Molecular Probes) dye. Once the cytosolic DHE is oxidized to ethidium, it is intercalated into the cell's DNA, staining its nucleus a bright fluorescent red. Use of this dye to measure oxidative activity in endothelial cells is supported in the literature (Carter et al. 1994; De Keulenaer et al. 1998). The HAECs were incubated with 1, 10, and 50 µg/mL of Fe_2O_3, Y_2O_3, and ZnO nanoparticles as described previously. Control cells (without nanoparticles) were incubated at the same time. At the end of a 4-hour incubation, the cells were washed and incubated for 30 minutes at 37°C with 5 µM of DHE diluted in HBSS. We had determined the optimal dye concentration in previous optimization experiments.

The images were acquired on an inverted microscope (Nikon Eclipse TE300, Melville, NY) equipped with a Retiga charge-coupled device (CCD) camera (QImaging, Surrey, BC). SimplePCI imaging software (Compix, Cranberry Township, PA) was then used to capture the images on a computer.

We also evaluated expression of the genes heme oxygenase 1 (HMOX1), glutamate-cysteine ligase (GCLC), and nicotinamide adenine dinucleotide phosphate (NADPH) oxidase 4 (NOX4). The HAECs were incubated with 1 and 10 µg/mL Fe_2O_3, Y_2O_3, and ZnO nanoparticles as described previously. After isolation of RNA and preparation of cDNA, quantitative real-time PCR was performed. Human GAPDH was used as an internal control. Primers for these markers were designed by Primer Express and purchased from Operon Technologies. Their sequences were as follows:

HMOX1 antisense:5′-CAGCCCTCTCACTGTGTCCC-3′
HMOX1 sense:5′-GCCATAGGCTCCTTCCTCCTT-3′
GCLC antisense:5′-AGCTGTTGCAGGAAGGCATT-3′
GCLC sense:5′-GATGAGCAACATGCTGGGC-3′
NOX4 antisense:5′-CAACTGTTCCTGGCCTGACA-3′
NOX4 sense:5′-TGAGGAATAGCACCACCACCA-3′

DATA ANALYSIS

In the figures that follow, data are presented as means ± SE. Statistical analyses were performed by one-way ANOVA followed by the Dunnett post-hoc test. Differences in means were considered significant if $P < 0.05$.

RESULTS

CHARACTERISTICS OF PARTICLES

Representative TEM images of the Fe_2O_3, Y_2O_3, and ZnO nanoparticles are shown in Figure 2. XRD and TEM analysis revealed that the Fe_2O_3 nanoparticles exhibited the crystal structure of γ-Fe_2O_3, or maghemite, and can be divided into two groups according to size—one group in the range of 30 to 90 nm and the other consisting of particles smaller than 5 nm (Figure 2 top panel). The Y_2O_3 nanoparticles have a C-type cubic structure and are present as aggregates with primary particle sizes in the range of 20 to 60 nm (Figure 2 middle panel). The ZnO nanoparticles have a zincite crystal structure and are rod-shaped, with lengths ranging from 100 to 200 nm and diameters ranging from 20 to 70 nm (Figure 2 bottom panel). The specific surface areas measured with the BET technique for the Fe_2O_3, Y_2O_3, and ZnO nanoparticles

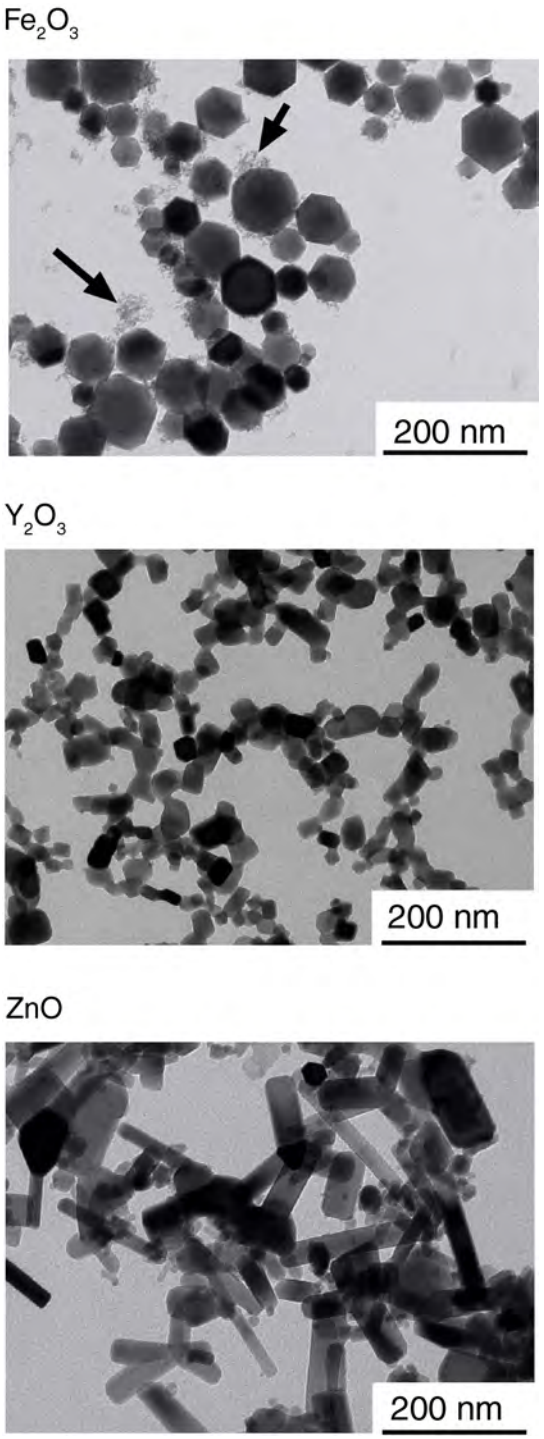

Figure 2. TEM images of metal oxide nanoparticles. In the top panel, arrows point to the subpopulation of Fe_2O_3 particles smaller than 5 nm.

were 81 ± 1, 41 ± 1, and 20.8 ± 0.2 m^2/g respectively. The smaller size range present in the case of Fe_2O_3 nanoparticles was not evident in the TEM images of the Y_2O_3 or ZnO particles. The particle-size distribution of the Y_2O_3 and ZnO particles was not measured using the SMPS because of the difficulty in diluting the flame-generated aerosols.

Although some of the particles in Figure 2 appear to be aggregates, it is difficult to infer the state of aggregation of particles from the TEM images. When the TEM images were acquired, samples of particles were dispersed in suspension and then dropped onto TEM grids and dried. This process inevitably leads to the appearance of aggregates as the sample dries; however, caution is required in interpreting the images as indicative of aggregation in the dispersed phase. As noted in the Materials and Methods section, particle stock solutions were sonicated for 5 minutes before the final working concentrations were prepared, to minimize the possible presence of aggregates. It is likely, however, that some agglomeration of particles does take place during the course of exposure of cells, even after dispersion with a sonicator.

Consistent with the TEM images, the SMPS analysis demonstrated that Fe_2O_3 particles fell into two size ranges. Particles in the larger range are nonagglomerated, are nearly spherical, and appear to have a log-normal size distribution. Based on the SMPS and TEM surveys, the count median diameter (CMD) of the particles in the log-normal size distribution is approximately 45 nm, with a geometric standard deviation (GSD) of approximately 1.2. The particles in the smaller range are nearly monodisperse with an estimated mean diameter of approximately 5 nm. The smaller particles probably arise from nucleation of fresh particles from the gas phase in the highest temperature zone of the flame. Our SMPS could not resolve the smaller range of the Fe_2O_3 particle-size distribution. Hence, to infer the contribution of each size range to the particle number, surface area, and mass of the combined bimodal aerosol, we resorted to measuring direct physical surface areas of the particles using the BET method and analyzing the resolved size distribution of the larger particles. The ratio of the particle-number concentration of the smaller range to particle-number concentration of the larger range was calculated using the following equation:

$$\frac{\pi}{6}\left[d^3_{\bar{m}\_Large} + d^3_{Small} R_{S/L}\right]\rho\left(\frac{S}{M}\right)_{\mathrm{BET}} = \pi\left[d^2_{\bar{s}\_Large} + d^2_{Small} R_{S/L}\right]$$

where $d_{\bar{m}\_Large}$ is the diameter of particles with average mass for the larger range, which, calculated from the CMD and GSD of the assumed log-normal distribution (Hinds 1999), is approximately 47 nm; $d_{\bar{m}\_Small}$ is the estimated diameter of the smaller-range particles, assumed to be monodispersed, approximately 5 nm; $R_{S/L}$ is the ratio of the number concentration of the smaller-range particles to the number concentration of the larger ones; $(S/M)_{\mathrm{BET}}$ is the value of the BET-derived specific surface area measurement for the Fe_2O_3 particles (large and small ranges both included), 81 ± 1 m^2/g; $d_{\bar{s}\_Large}$ is the diameter of particles with average surface area for the larger range, which is approximately 47 nm, as calculated from the CMD and GSD of the assumed log-normal distribution. With the reasonable assumption of a log-normal distribution for the larger range of particles and a monodisperse distribution for the smaller range of particles, the equation can be solved to yield a value of approximately 330 for $R_{S/L}$, indicating that for every particle in the larger range, there are approximately 330 particles in the smaller range. The results also indicate that the smaller-range particles account for approximately 28% of the particle mass and approximately 79% of the particle surface area.

The in situ geometric mean diameter (GMD) of CeO_2 particles measured with SMPS ranged from 28 to 38 nm at different heights above the burner. BET measurements of the surface area showed the GMD to be about 19 m^2/g. By assuming a bulk density of 7.2 g/cm^3 and a spherical shape for the CeO_2 particles, the equivalent diameter was calculated to be 44 nm, which agrees well with the SMPS measurement. TEM measurements were performed using a low-magnification TEM (the high-magnification TEM was under repair on campus). The quality of the images was not satisfactory, however, so they are not presented. XRD analysis showed that the CeO_2 crystal size was about 3 nm and about 7 nm for the O_2 and N_2 co-flow cases, respectively, leading to the conclusion that the crystal domain size was affected by the flame temperature. The crystals were much smaller than the particles, indicating that the CeO_2 particles were polycrystalline. The XRD patterns of all the samples, which varied depending on the co-flow gas used and therefore flame temperature, were consistent with CeO_2. We could not find a signature for other phases of CeO_2 such as Ce_2O_3. We also dissolved particle samples in 3% HNO_3 and analyzed them with ICP–MS, which confirmed the purity of the particles: Cerium was the only measurable metal within our limits of detection.

UPTAKE OF PARTICLES

ICP–MS measurements revealed that the amount of metal taken up (g/cell) correlated directly with the concentration of metal oxide in the extracellular solution for all

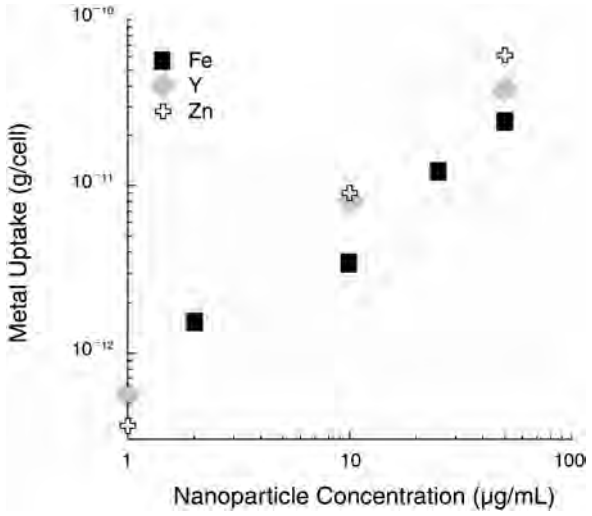

Figure 3. ICP–MS measurements of uptake by HAECs of the three different types of nanoparticles as a function of the metal oxide concentration in the extracellular solution.

three types of nanoparticles (Figure 3). These results indicate a clear, dose-dependent pattern of uptake of the metal oxide nanoparticles by HAECs and show that the nanoparticle concentration within the cell culture medium provides an accurate measure of the particle dose delivered to the cell surface.

Thin-section TEM images show that after a 4-hour incubation, Fe_2O_3 nanoparticles at all concentrations tested (0.001–50 µg/mL) were incorporated into HAECs; the number of nanoparticles in cells increased with concentration. Identification of Fe_2O_3 nanoparticles inside the cells was straightforward since the particles remained faceted. The Fe_2O_3 nanoparticles were often present within cytoplasmic vesicles (white areas containing metal oxide particles) (Figure 4, top-left image). No substantial swelling was observed in the vesicles containing Fe_2O_3 nanoparticles. Swelling in the presence of Y_2O_3 and ZnO particles might suggest that the cells struggled to maintain lysosomal pH.

Objects with high electron density were found in the thin-section TEM images of HAECs treated with Y_2O_3 nanoparticles. As with Fe_2O_3 nanoparticles, these objects were often present within cytoplasmic vesicles (Figure 4, top-right image), and their density increased with nanoparticle concentration. Although they did not have the characteristic morphology of the original Y_2O_3 nanoparticles (see Figure 2), and although elemental analysis was not performed to confirm their chemical composition, these high-electron-density objects were presumed to be the products of the degradation of the Y_2O_3 nanoparticles, as no other elements of comparable electron density should have been present in these thin sections and the objects were not observed in the control sample (Figure 4, bottom-right image). The vesicles containing these objects exhibited considerable swelling, particularly at the higher Y_2O_3 nanoparticle concentrations (Figure 4).

Thin-section TEM images of HAECs treated with 50 µg/mL ZnO nanoparticles showed fewer intracellular vesicles and high-electron-density particulate matter in the vicinity of the cell membrane (Figure 4, bottom-left image). Such particulate matter was not seen in the control (untreated) cells (Figure 4). In some instances, apparent discontinuities in the cell membrane were observed in HAECs treated with ZnO nanoparticles.

We studied the time course of nanoparticle uptake. HAECs were exposed to Fe_2O_3 particles (10 µg/mL solution) for 10, 30, and 60 minutes, and 4 hours. Uptake and transport were analyzed using TEM. In 30 minutes, Fe_2O_3 aggregates interacted with plasma membrane structures and were visible near surface invaginations with ultrastructural characteristics of caveolae (Figure 5, top panel). At 4 hours the accumulation of electron-dense particles in intracytoplasmic vacuoles was accompanied by exocytosis of particles on the basilar surface (Figure 5, bottom panel). Our results showed that metal oxide nanoparticles were internalized and transported across endothelial cell membranes.

EFFECT OF NANOPARTICLES ON HAEC INFLAMMATION AND VIABILITY

Incubating HAECs for 4 hours with Fe_2O_3 nanoparticles did not induce an increase in ICAM-1, IL-8, or MCP-1 mRNA levels relative to control cells (Figure 6, top-left panel). For instance, the ICAM-1, IL-8, and MCP-1 mRNA levels of HAECs incubated with 50 µg/mL Fe_2O_3 nanoparticles were 0.8 ± 0.2, 0.8 ± 0.2, and 0.7 ± 0.1 times the control values, respectively ($P > 0.05$).

Four-hour incubation with Y_2O_3 nanoparticles induced a significant increase in ICAM-1, IL-8, and MCP-1 mRNA levels. The effect of Y_2O_3 nanoparticles depended on concentration, and a statistically significant increase occurred at the two highest concentrations—10 and 50 µg/mL (Figure 6, top-right panel). At 50 µg/mL, Y_2O_3 nanoparticles increased ICAM-1, IL-8, and MCP-1 mRNA levels relative to control cells by 5.3 ± 0.6, 3.3 ± 0.5, and 6.8 ± 1.6 times, respectively ($P < 0.05$ for all three markers). At 10 µg/mL, the equivalent mRNA up-regulation values were 2.2 ± 0.3, 1.2 ± 0.3, and 2.2 ± 0.1 for ICAM-1, IL-8, and MCP-1, respectively ($P < 0.05$ for ICAM-1; $P > 0.05$ for MCP-1 and IL-8).

ZnO nanoparticles also elicited an inflammatory reaction in HAECs in a concentration-dependent manner

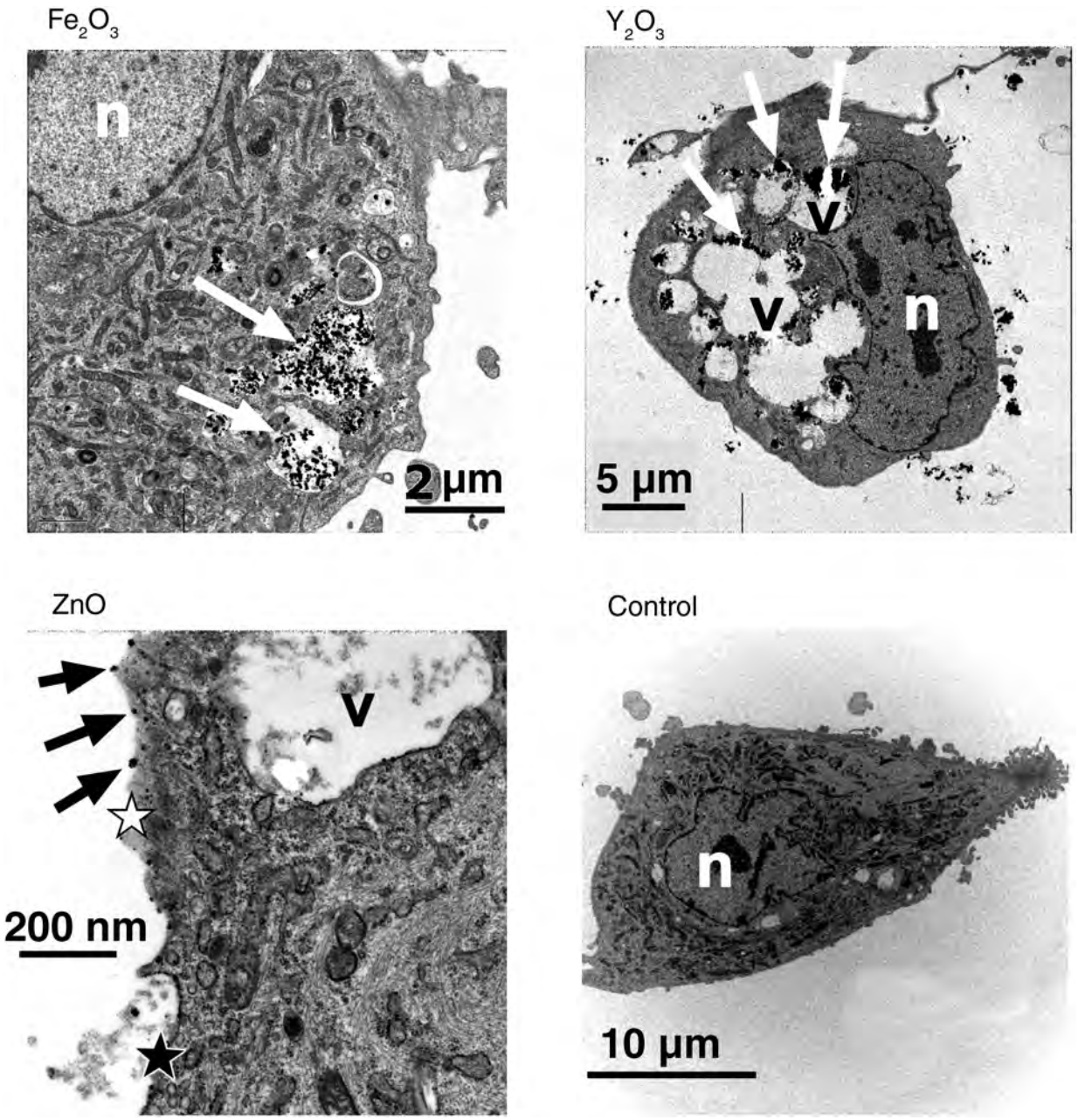

Figure 4. Thin-section TEM images of HAECs incubated with metal oxide nanoparticles. n: nucleus; v: vesicle; black star with white border: normal continuous cell membrane; white star: region of possible cell membrane discontinuity; arrow: points to metal oxide particles.

(Figure 6, bottom-left panel). At 50 µg/mL, ICAM-1, IL-8, and MCP-1 mRNA levels increased relative to control cells by 13.6 ± 4.1, 6.4 ± 2.5, and 10.8 ± 6.2 times, respectively ($P < 0.05$ for ICAM-1 and IL-8; $P > 0.05$ for MCP-1). The equivalent values for 10 µg/mL were 17.9 ± 2.1, 5.2 ± 2.2, and 4.0 ± 0.6 ($P < 0.05$ for ICAM-1; $P > 0.05$ for MCP-1 and IL-8).

Incubation of HAECs with CeO_2 nanoparticles gave rise to a small increase in inflammatory markers at the two highest concentrations—10 and 50 µg/mL (Figure 6, bottom-right panel). A dose of 10 µg/mL of CeO_2 nanoparticles increased mRNA up-regulation of ICAM-1, IL-8, and MCP-1 by 1.1 ± 0.1, 1.4 ± 0.2, and 1.4 ± 0.4 times, respectively, in comparison with the control cells ($P > 0.05$). A dose of

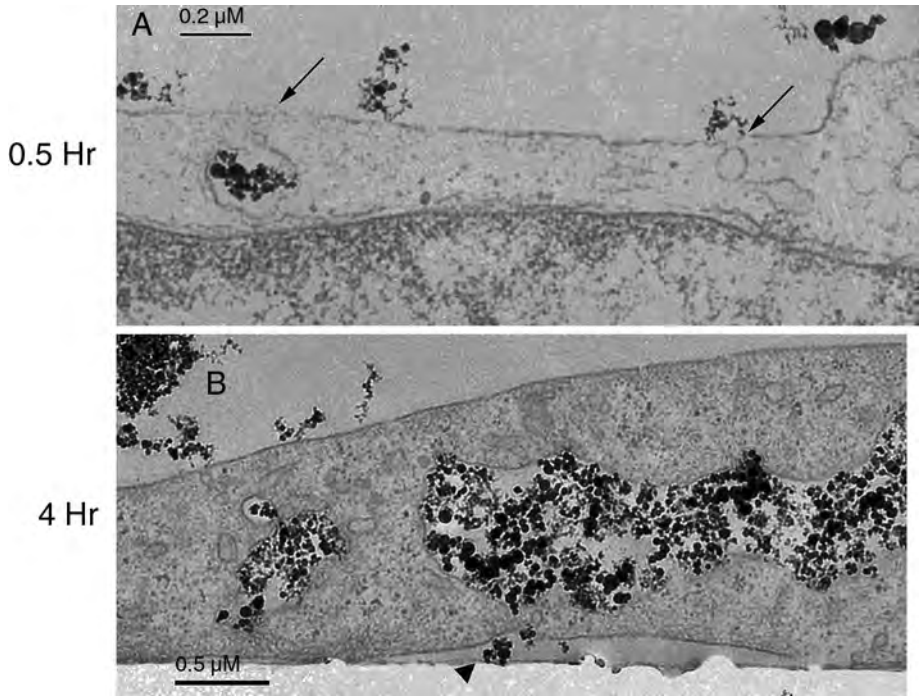

Figure 5. TEM images of HAEC cell cultures exposed to 10 μg/mL Fe_2O_3 particles. Top panel: After 0.5-hour incubation, aggregates of particles accumulate near surface invaginations with ultrastructural characteristics of caveolae (indicated by arrows). **Bottom panel:** By 4 hours of incubation, the accumulation of particles in intracytoplasmic vacuoles is accompanied by exocytosis of particles on the basilar surface, indicated by the arrowhead.

50 μg/mL increased mRNA up-regulation of the same markers by 1.4 ± 0.3, 1.8 ± 0.5 ($P < 0.05$), and 2.0 ± 0.6 times ($P > 0.05$), respectively. No difference was found at the lower concentrations tested. Despite slight mRNA up-regulation of inflammatory markers caused by higher concentrations of CeO_2 nanoparticles, the increase was lower than what was seen for Y_2O_3 nanoparticles, and there was no statistically significant effect.

ZnO nanoparticles had the most striking effect on HAECs (Figure 6, bottom-left panel). At the two highest concentrations, ZnO nanoparticles provoked considerable detachment at the end of the 4-hour incubation period (most occurring during the last hour of incubation). This was unlike the effects of the presence of Fe_2O_3 and Y_2O_3 nanoparticles, which did not lead to visible cell loss after 4 hours of incubation. At 50 μg/mL, cell loss after the 4-hour ZnO incubation was approximately 50 to 60%; it was approximately 20% at 10 μg/mL. No cell loss was noted at the lower concentrations. HAECs that remained attached after incubation with ZnO nanoparticles showed viability rates that were similar, as assessed by trypan blue exclusion, to those of control cells and cells exposed to Fe_2O_3 and Y_2O_3 nanoparticles. More specifically, HAEC viability rates (in three separate experiments) after the 4-hour incubation were as follows ($P > 0.05$ relative to the control in all cases): 88 ± 1% for control cells; 89 ± 1% and 82 ± 3% for cells exposed to ZnO nanoparticles at 10 and 50 μg/mL, respectively; 88 ± 2% and 88 ± 4% for cells exposed to Y_2O_3 nanoparticles at 10 and 50 μg/mL, respectively; and 88 ± 4% and 92 ± 3% for cells exposed to Fe_2O_3 nanoparticles at 10 and 50 μg/mL, respectively. Largely similar viability rates were obtained after 8 hours of incubation.

To assess the longer-term impact of ZnO nanoparticles on HAEC viability, cells were incubated with these particles at either 10 or 50 μg/mL for 4 hours, washed with PBS (3 times), and then maintained for another 24 hours in cell culture medium free of nanoparticles. Although this protocol did not lead to a significant decrease in cell viability at 10 μg/mL (89 ± 2% versus 90 ± 1% for control cells; $n = 4$, $P > 0.05$), viability significantly decreased at 50 μg/mL (71 ± 7%; $n = 4$, $P < 0.05$ relative to the control). We note, however, that there were technical difficulties associated with the protocol. We found it very difficult to remove all particles from the cell surface by washing, especially at the higher particle concentrations. Therefore, the particles that remained attached after washing may have continued to influence cell viability during the ensuing 24-hour period.

To elucidate the temporal evolution of transcriptional inflammatory changes induced by Fe_2O_3, CeO_2, and Y_2O_3 nanoparticles, we studied ICAM-1, IL-8, and MCP-1 mRNA

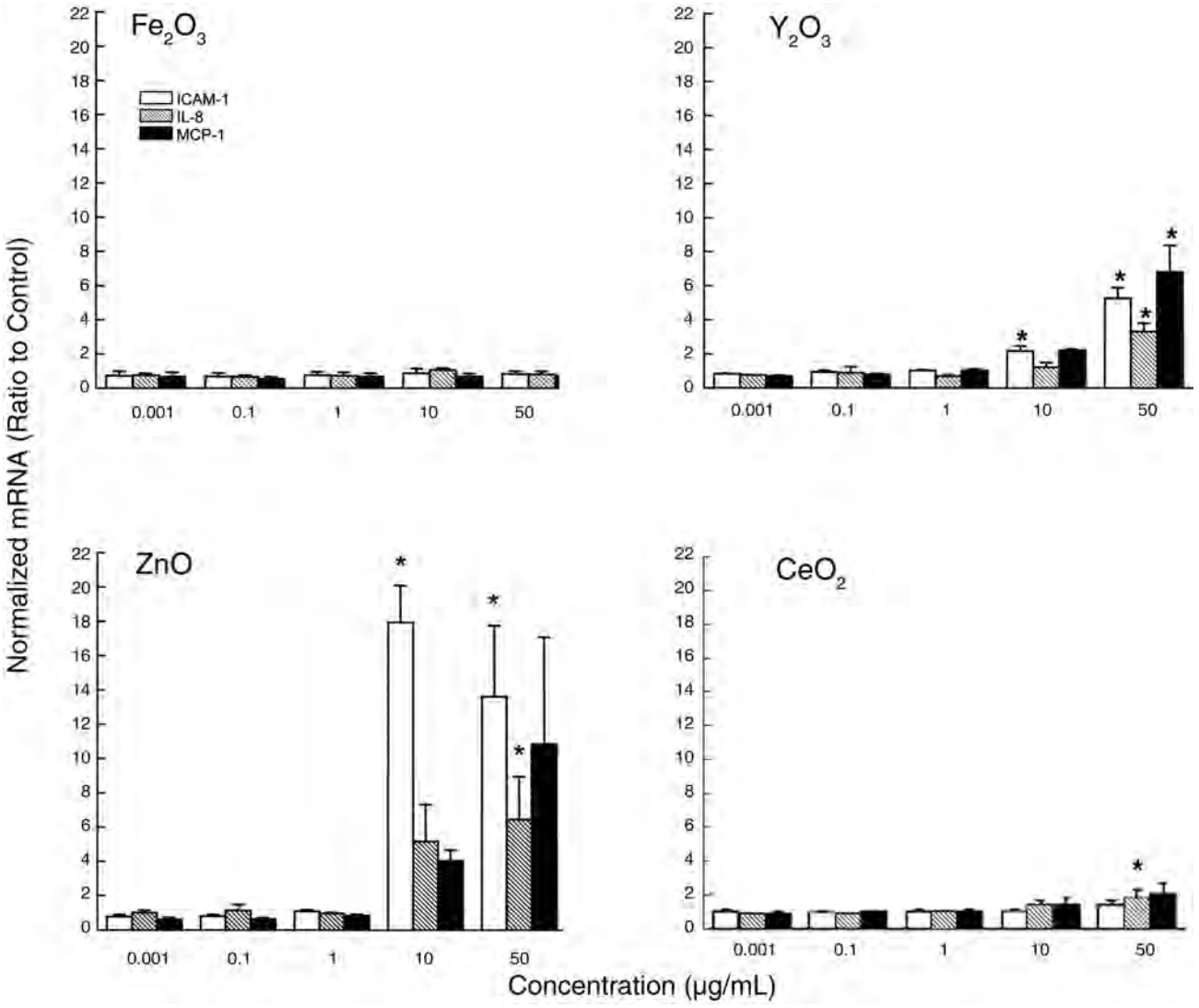

Figure 6. mRNA levels of the three inflammatory markers ICAM-1, IL-8, and MCP-1 in HAECs incubated for 4 hours with metal oxide nanoparticles. Each mRNA value was normalized to the corresponding GAPDH value. The values shown for mRNA are ratios relative to control cells (with no nanoparticles present). Data are means ± SE from three independent experiments. An asterisk denotes a statistically significant increase in the mRNA level compared with control cells ($P < 0.05$).

levels at three additional time points: 1, 2, and 8 hours. Because the 4-hour data had demonstrated that the critical concentration threshold for inducing an inflammatory response was between 1 and 10 μg/mL (see Figure 6), these two concentrations were selected for the experiments at the additional time points. At the 1- and 2-hour time points, only ZnO nanoparticles at a concentration of 10 μg/mL increased ICAM-1, IL-8, and MCP-1 mRNA levels significantly (Figure 7, left and middle panels). At 8 hours, these increases persisted, though at a lower level. There was also a modest increase at 8 hours in ICAM-1 and MCP-1 mRNA levels in HAECs incubated with Y_2O_3 nanoparticles at a concentration of 10 μg/mL (Figure 7, right panel). Fe_2O_3 nanoparticles did not elicit an inflammatory response at any of the time points or concentrations tested.

Although ZnO nanoparticles increased the mRNA levels of all three inflammatory markers, the dynamics of this increase were different for the different markers. While ICAM-1 mRNA levels increased between the 1- and 2-hour time points and remained elevated at 8 hours, IL-8 and MCP-1 mRNA expression peaked at 2 hours and then decreased to considerably lower levels (though significantly higher than control levels) at the 4- and 8-hour time points, as seen in Figures 6 and 7.

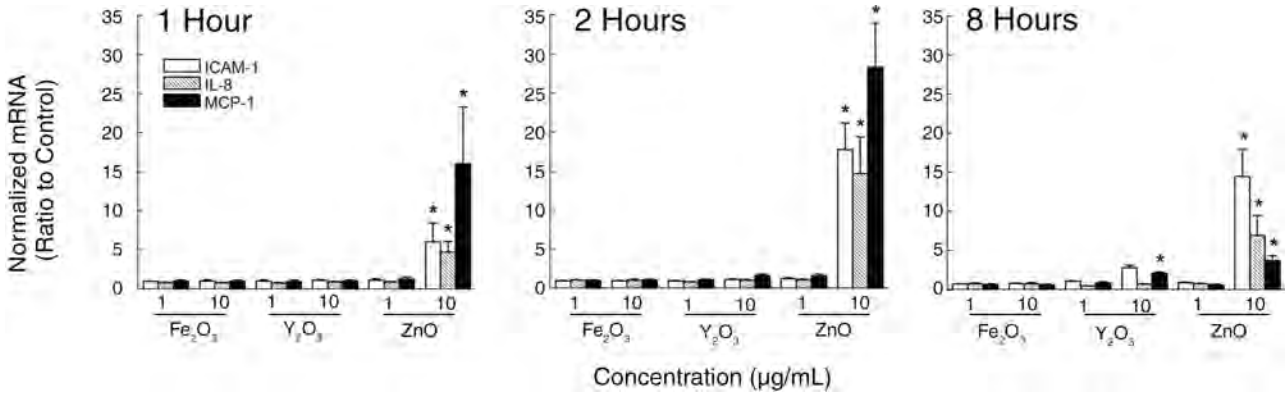

Figure 7. mRNA levels of the three inflammatory markers ICAM-1, IL-8, and MCP-1 in HAECs incubated with nanoparticles (1 and 10 μg/mL concentrations). Each mRNA value was normalized to the corresponding GAPDH value. The values shown for mRNA are ratios relative to control cells (with no nanoparticles present). Data are means ± SE from three independent experiments. An asterisk denotes a statistically significant increase in the mRNA level compared with control cells ($P < 0.05$).

In addition to the transcriptional response, the upregulation of inflammatory markers by nanoparticles was also observed at the translational, or protein, level (Figure 8). We used Western blot analysis (Figure 8, panel A, top) to determine levels of ICAM-1 protein in HAECs after 4-hour incubation with nanoparticles. The values in panel A are normalized to β-actin as an internal control rather than the assay control (untreated cells), which is why the control value is not 1.0. Fe_2O_3 and Y_2O_3 nanoparticles did not increase ICAM-1 protein at any of the concentrations tested. By contrast, ZnO nanoparticles at 10 and 50 μg/mL increased ICAM-1 protein levels relative to control cells by 1.8 ± 0.5 and 2.2 ± 0.6 times, respectively ($P = 0.06$ and $P < 0.05$, respectively). We used an ELISA to test MCP-1 protein concentrations in cell culture supernatants of HAECs incubated with nanoparticles for 4 hours. In line with the mRNA results, Fe_2O_3 nanoparticles did not elicit an increase in MCP-1 protein levels relative to control cells (Figure 8, panel B). In this figure, the data are normalized to the control of the assay (untreated cells), so no control value is present in the graph. At 10 and 50 μg/mL, Y_2O_3 nanoparticles increased MCP-1 protein levels relative to control cells by 1.5 ± 0.1 and 3.2 ± 0.5 times, respectively ($P > 0.05$ for both comparisons). Similar concentrations of ZnO nanoparticles increased MCP-1 protein concentrations by 8.0 ± 1.1 and 6.8 ± 1.2 times ($P < 0.05$ for both). There was no significant increase in MCP-1 protein levels at the 1 μg/mL concentration of Fe_2O_3, Y_2O_3, or ZnO nanoparticles.

ROLE OF RELEASED METALS AND HAEC INFLAMMATION

A question that arises is whether the inflammatory response is due at least in part to the release of reactive metal species from the nanoparticles. To address this issue, we performed limited experiments in which cell culture medium that was incubated for 4 hours with Fe_2O_3, Y_2O_3, or ZnO nanoparticles (at either 10 or 50 μg/mL) was centrifuged to remove most nanoparticles. After that the supernatant was added to the HAECs for another 4 hours. For all three types of nanoparticles, ICAM-1, IL-8, and MCP-1 mRNA levels were virtually identical to those of control cells (data not shown). These findings suggest that the inflammatory response we observed was due to the presence of the particles, rather than to reactive metals that may have been released into the growth medium.

IDENTIFICATION OF SUBCELLULAR COMPARTMENTS CONTAINING PARTICLES

Our original proposal was to use Europium-tagged particles for colocalization studies of intracellular transport pathways. In our initial attempt, we found that under confocal microscopy the intensity of fluorescence of these particles was suboptimal in application relative to the intensity of the subcellular markers, at least with the microscope that was available at the time. We have very recently found that a newer confocal microscope on campus has laser excitation lines that work well with the Europium-tagged particles and that allow us to see the particles within cells. We have also used silicon dioxide (SiO_2) particles that contain fluorescein isothiocyanate (FITC) dye for comparison—they are also visible inside and outside of the cell membranes of the HAECs under the confocal microscope. These results are very preliminary, and we have not determined the distribution of the particles in cells by imaging in the Z direction; imaging in this direction would allow us to determine if the particles are on the cell surfaces or are internalized.

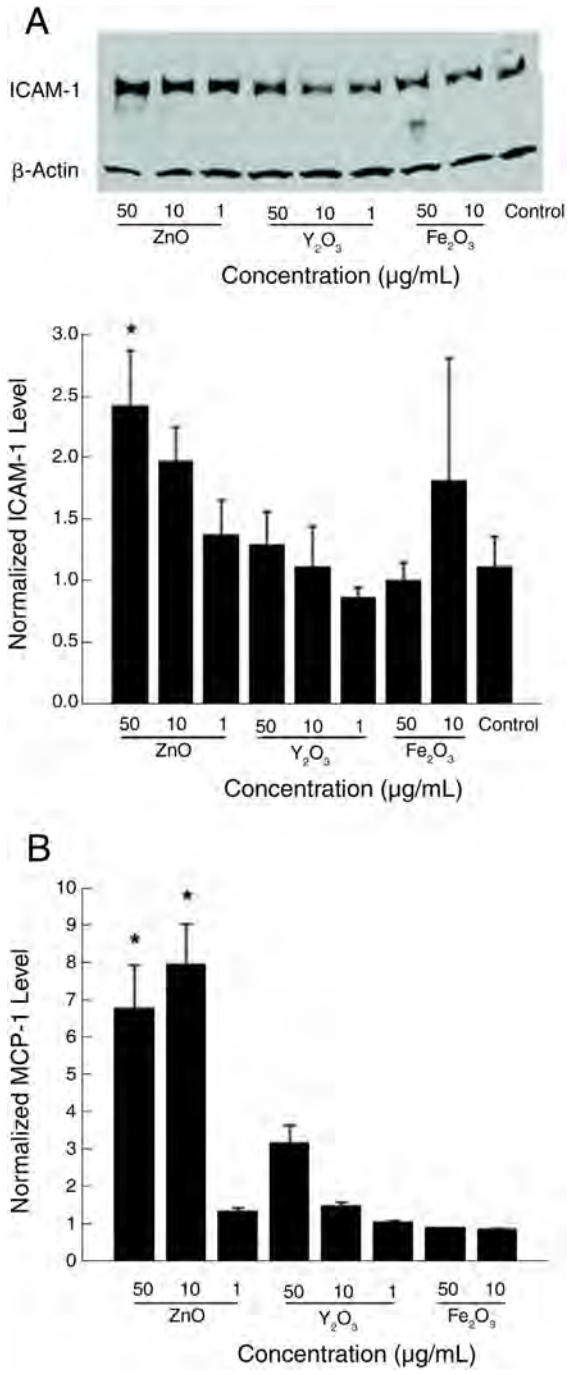

Figure 8. Levels of ICAM-1 and MCP-1 proteins in HAECs incubated with nanoparticles for 4 hours (at 1, 10, and 50 μg/mL concentrations). ICAM-1 levels were determined by Western blot analysis, and MCP-1 levels were obtained using ELISA. **A:** Representative Western blot and densitometric analyses of ICAM-1 protein levels. ICAM-1 band densities have been normalized to the internal control (β-actin). Data are means ± SE from 3 to 6 independent experiments. **B:** ELISA results for MCP-1 levels relative to control cells (with no nanoparticles present). Data are means ± SE from 3 to 4 independent experiments. An asterisk denotes a statistically significant increase in the protein level compared with control cells ($P < 0.05$).

DETECTION OF INTRACELLULAR OXIDATION

We compared the effects of particles composed of Fe_2O_3, ZnO, Y_2O_3, and National Institute of Standards and Technology (NIST) standard urban particles with soluble Fe_2O_3 and medium as well as 1% H_2O_2. Each particle form was administered as a 1 or 10 μg/mL concentration in medium. We found CM-H_2DCFDA fluorescence to be an insensitive assay in HAECs. Only modest fluorescence was detected with the H_2O_2 treatment, our positive control. We were able to demonstrate significant increases in CM-H_2DCFDA fluorescence after 2 hours with the higher concentration of the NIST sample, while the results of other treatments were not distinguishable from those of the medium control. The increase in the fluorescence of the NIST sample at 2 hours was statistically significant by ANOVA with a Sheffé post-hoc test. A qualitatively similar but not statistically significant increase in fluorescence occurred in cultures after 4 hours. In part, the lack of sensitivity appeared to relate to a high background CM-H_2DCFDA fluorescence, as cultures not preloaded with CM-H_2DCFDA had only 50% of the integrated density found in preloaded cultures incubated in medium alone (data not shown). Note that we have demonstrated a significant CM-H_2DCFDA signal using the redox cycling agent naphthoquinone in related experiments (unpublished observations; manuscript in preparation) with pulmonary artery endothelial cell cultures.

When we examined the nuclear translocation of Nrf2, we found qualitatively increased translocation in the 10 μg/mL concentrations of NIST standard urban particles, Y_2O_3, and ZnO, but these differences were not statistically different from those for the control cultures. No increase in Nrf2 translocation was evident in cells treated with Y_2O_3 particles.

In the DHE staining assay, we noted increased nuclear fluorescence in HAECs treated with 10 and 50 μg/mL ZnO and 50 μg/mL Y_2O_3 nanoparticles (Figure 9). The majority of the nuclei of cells treated with 50 μg/mL ZnO nanoparticles showed increased fluorescence (Figure 9, A, left image). When 10 μg/mL of the same nanoparticles was applied to the HAECs, only some cells seemed to produce ROS (Figure 9, B, left image). The same was true for cells treated with 10 μg/mL of Y_2O_3 nanoparticles (Figure 9, B, middle image). Cells treated with Fe_2O_3 nanoparticles had virtually the same degree of fluorescence as the control cells (Figure 9). Treating cells with 1 μg/mL of any of the three kinds of nanoparticles did not lead to increased fluorescence in comparison with control cells (data not shown). As a positive control, we again used HAECs treated with H_2O_2, which is known to induce ROS production (Figure 9, C, right image). Qualitatively, 10 minutes of treatment with 10 mM of H_2O_2 produced amounts of ROS similar

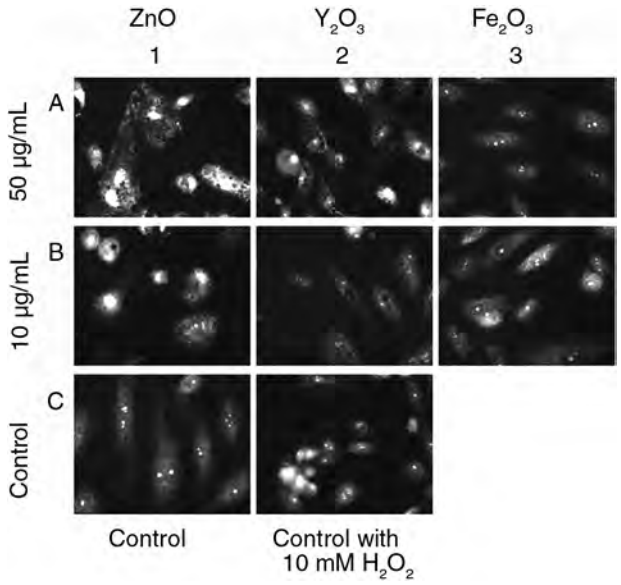

Figure 9. Images of HAECs incubated with nanoparticles or medium alone for 4 hours followed by DHE staining for 30 minutes. Magnification 400×.

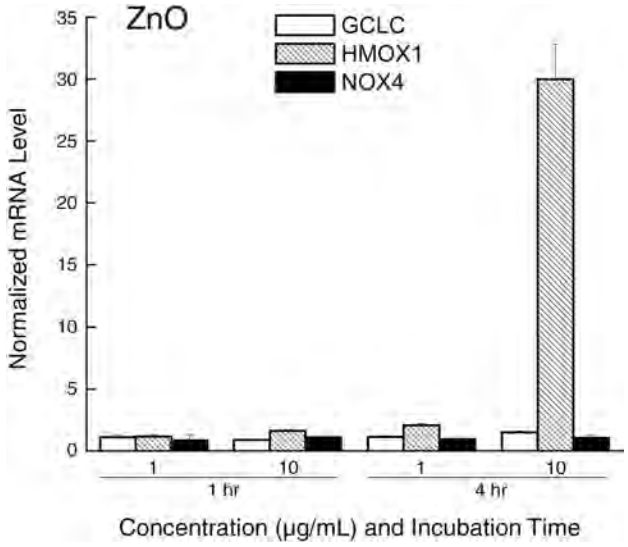

Figure 11. mRNA levels of the three oxidative markers GCLC, HMOX-1, and NOX4 in HAECs incubated with 1 or 10 µg/mL of ZnO nanoparticles for 1 or 4 hours. Each mRNA value was normalized to the corresponding GAPDH value. The values shown for mRNA are ratios relative to control cells (with no nanoparticles present). Data from one experiment are shown.

to those produced by 4-hour treatments with 10 µg/mL ZnO or 50 µg/mL Y_2O_3 nanoparticles. HAECs treated with 50 µg/mL of ZnO nanoparticles led to even higher ROS production. We need to emphasize, however, that the treatment with 10 mM H_2O_2 produced a sudden and significant death of cells, and as a result, no quantification was performed. Any comparisons are only approximate.

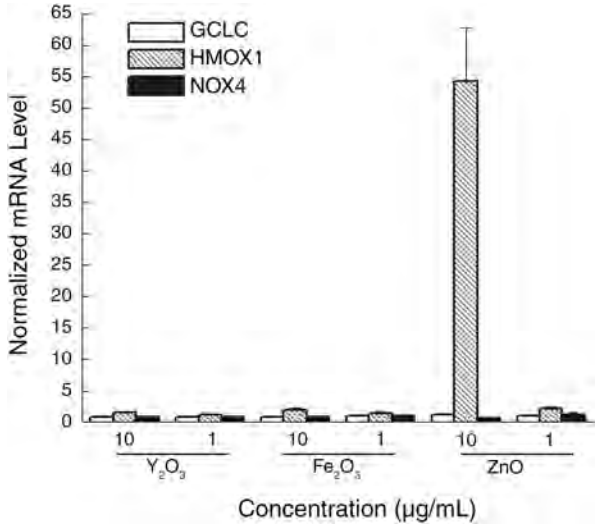

Figure 10. mRNA levels of the three oxidative markers GCLC, HMOX1, and NOX4 in HAECs incubated for 4 hours with 1 or 10 µg/mL of Fe_2O_3, Y_2O_3, and ZnO nanoparticles. Each mRNA value was normalized to the corresponding the GAPDH value. The values shown for mRNA are ratios relative to control cells (with no nanoparticles present). Data from one experiment are shown.

These data show that production of ROS and increased up-regulation of inflammatory markers in response to ZnO and Y_2O_3 nanoparticles occurs in the same time frame. Therefore, it may be possible that increased inflammation is related to the generation of ROS. However, future studies using shorter incubation time points will be needed before any final conclusions can be drawn.

As indicators of ROS generation, we measured mRNA levels of GCLC, HMOX1, and NOX4 after a 4-hour incubation with nanoparticle concentrations of 1 and 10 µg/mL. Of the three different kinds of particles that we tested, only ZnO showed an effect on expression of those genes (Figure 10). The cells incubated with 10 µg/mL of ZnO nanoparticles showed a significant increase of HMOX1, to a level 54 times that in control cells. Because oxidative stress is believed to occur soon after an insult, we measured transcription levels at the very early time point of 1 hour: Incubation of HAECs with ZnO nanoparticles for 1 hour did not lead to an increase in mRNA expression. Only an incubation time of 4 hours (Figure 11) resulted in an increase in the level of HMOX1 mRNA.

DISCUSSION

The mechanisms governing the epidemiologic correlation between exposure to nanoparticles and an increased

incidence of cardiovascular disease remain to be elucidated. Because induction of an endothelial inflammatory response is a critical early event in vascular pathology, we studied the effects of nanoparticles on inflammation in HAECs. Our results demonstrate that direct and acute exposure of HAECs to Y_2O_3 or ZnO nanoparticles significantly up-regulates mRNA levels of the inflammatory markers IL-8, ICAM-1, and MCP-1, whereas Fe_2O_3 nanoparticles have no effect and CeO_2 particles have a barely significant effect. In general, the extent of mRNA up-regulation was greater for ZnO than for Y_2O_3. Whenever it occurred, the inflammatory response was not evident below a particle concentration of approximately 10 μg/mL and was dose dependent above this threshold concentration. At the highest concentrations tested (50 μg/mL), ZnO nanoparticles led to considerable cell toxicity in addition to the pronounced inflammatory response.

A key finding of the present study is that the composition of nanoparticles is a major determinant of their propensity to induce inflammation in HAECs; however, the mechanism for this effect is not known. At this point, it remains unknown if the degree of endothelial inflammation caused by nanoparticles of different compositions applies only to metal oxide particles or is a more general phenomenon. In any case, this dependence is not attributable to differences in the ability of the different types of particles to access the endothelial surface or to enter the intracellular space. Our results show that Fe_2O_3, Y_2O_3, and ZnO nanoparticles are internalized within HAECs and that a given particle concentration in the cell culture medium leads to the delivery of a related dose to the cells. Therefore, it is likely that the (specific) composition of metal oxide nanoparticle influences the signaling pathways that activate the inflammatory response.

Interestingly, the extent of inflammatory responses in HAECs appears to correlate inversely with the specific surface area of nanoparticles, although this issue needs to be addressed more systematically in future studies. ZnO nanoparticles, which have the smallest specific surface area, are associated with the most pronounced inflammatory response. Our results demonstrate that Fe_2O_3 nanoparticles do not elicit inflammation; these particles have the largest specific surface areas among the three types of particles for which surface areas were obtained by BET measurement (CeO_2 was not included). At a minimum, it appears that surface area is not a good indicator of inflammation for the four materials that we have examined.

To observe effects within 4 to 8 hours, we found that it was necessary to work with concentrations of at least 1 to 10 μg/mL. These in vitro concentrations are significantly greater than concentrations that might be expected from actual inhalation exposure to the same material. The results, however, are useful in determining the potentials of a range of relevant metal oxides for initiating inflammation in HAECs.

We determined that the possible release of ROS from the nanoparticles does not contribute substantially to the inflammatory response in HAECs. This result is consistent with previous findings—although nickel and cobalt ions elicit the production of ICAM-1, E-selectin, IL-6, and IL-8 in human umbilical-vein endothelial cells (HUVECs) (Wagner et al. 1998), nickel nanoparticles have virtually no effect on HUVEC inflammation or toxicity (Peters et al. 2004). A recent study demonstrating that the release of soluble components is not responsible for the inflammatory properties of carbon black nanoparticles (Brown et al. 2000) further corroborates the notion that the impact of free metal release from nanoparticles on inflammation is minimal.

An obvious candidate pathway for nanoparticle-induced inflammation in HAECs is the production of ROS. Exposure to nanoparticles is generally thought to lead to ROS generation and cellular oxidative stress (Donaldson et al. 2001; Nel et al. 2006). However, a recent report has suggested that CeO_2 and Y_2O_3 nanoparticles act as antioxidants in neurons (Schubert et al. 2006). We tested the impact of Fe_2O_3, Y_2O_3, and ZnO nanoparticles (1, 10, and 50 μg/mL for 2 and 4 hours) on ROS levels in HAECs using the fluorescent indicator CM-H_2DCFDA. Visual inspection of the images could not positively confirm the presence of ROS; quantification of these results proved difficult due to the high background fluorescence in the images. Further studies with more sensitive reagents are needed to definitively establish a link between ROS formation and the inflammatory responses that we observed, if in fact ROS are responsible.

We focused on Fe_2O_3, CeO_2, Y_2O_3, and ZnO nanoparticles as examples of metal oxides that are associated with environmental and occupational exposures. Huggins and colleagues (2000) analyzed the metal content of NIST Standard Reference Material (SRM) urban and diesel engine particulate matter. They found that potassium and calcium were the most abundant metals, in both types of samples, followed by iron and zinc. Yttrium is widely used in catalysts and is also used as a host material for phosphors that are used in lighting and computer displays. Ceria is a commonly used catalyst. The oxides of the four metals also exhibit a range of properties, especially reactivity and solubility in acidic environments, that might be found in cytoplasmic vesicles in endothelial cells (Ollinger and Brunk 1995; Spragg et al. 1997). An interesting question that could be tested in future studies is whether differences in the propensity of different types of nanoparticles to induce endothelial inflammation relate to the reactivity of the metal oxides in acidic environments.

At the cellular level, much recent work has focused on using nanoparticles for targeted drug delivery and for visualizing intracellular processes (Panyam and Labhasetwar 2003; Pitsillides et al. 2003). These studies have investigated the uptake of nanoparticles by cells but have not addressed in detail the effect of nanoparticles on cellular pathology. A number of previous studies have demonstrated that exposure to nanoparticles induces inflammation in pulmonary epithelial cells and within the lung in general (Schaumann et al. 2004; Dagher et al. 2005). However, very few investigations have addressed the impact of nanoparticles on cardiac or vascular cells. Inhalation of particulate-matter-laden air has been shown to induce the release of endothelin-2 in rats (Elder et al. 2004). In vitro, incubation of HUVECs with particulate matter collected from air sampling has been reported to increase E-selectin production by 25% (Alfaro-Moreno et al. 2002). More recently, Peters and colleagues (2004) reported that direct exposure of dermal microvascular endothelial cells to metal nanoparticles decreased cellular viability and proliferation and induced IL-8 expression. Interestingly, the response was dependent on the composition of the nanoparticles—it was more pronounced for cobalt particles than for either SiO_2 or titanium dioxide (TiO_2) particles and was absent for nickel and polyvinyl chloride particles. Finally, a recent study (Yamawaki and Iwai 2006) demonstrated that carbon black nanoparticles (at concentrations of up to 100 μg/mL) altered the morphology of HUVECs and increased MCP-1 protein levels in a dose-dependent fashion, similar to the results we obtained with the ZnO and Y_2O_3 nanoparticles in the present study.

CONCLUSIONS

Cultures of HAECs were dosed with nanoparticles of Fe_2O_3, Y_2O_2, CeO_2, and ZnO that were generated in a flame. The particles were free of all detectable impurities. The average size of the particles was similar in all cases, but the surface area per unit mass was lowest for ZnO. Our data indicate that nanoparticle delivery to the HAEC surface and uptake within the cells correlate directly with the particle concentration in the cell culture medium.

HAECs treated with Fe_2O_3, Y_2O_2 and ZnO (but not CeO_2) nanoparticles were imaged with TEM. The particles were found to be internalized into HAECs. While the Fe_2O_3 and Y_2O_3 particles were found primarily within intracellular vesicles, ZnO particles localized in the vicinity of the cell membrane. Fe_2O_3 nanoparticles failed to provoke an inflammatory response in HAECs at any of the concentrations tested; however, Y_2O_3 and ZnO nanoparticles elicited a pronounced inflammatory response above a threshold concentration of about 10 μg/mL. At the highest concentration, ZnO nanoparticles led to considerable cell loss. CeO_2 caused a slight inflammatory response at the highest doses, substantially lower than that caused by Y_2O_3 or ZnO. These results demonstrate that the induction of inflammation in HAECs following acute exposure to metal oxide nanoparticles depends on particle composition and not just surface area.

We studied the effect of a broad range of nanoparticle concentrations on the inflammatory response of HAECs. The fraction of inhaled particles that ultimately cross the pulmonary epithelial barrier into the cardiovascular system is not known; therefore, the concentrations of particles to which endothelial cells are exposed in vivo remain to be determined. Some animal studies suggest that the particles that ultimately translocate to extrapulmonary organs amount to a small fraction (< 1%) of those deposited in the lungs (Kreyling et al. 2002). However, other studies have reported that about 10% to 15% of inhaled TiO_2 nanoparticles end up within the vascular compartment (Geiser et al. 2005). In a reported case of human zinc fume fever (Noel and Ruthman 1988), the serum zinc level rose from 1.1 to 1.6 μg/mL. If the excess zinc were in the form of ZnO particles, the increase would correspond to a ZnO concentration in the bloodstream of 0.5 μg/mL, which falls within the range of concentrations used in our study. Although this value falls below the threshold required to induce inflammation as reported here (approximately 10 μg/mL), it is essential to recognize that our study focused exclusively on short-term exposure (1–8 hours). The results of short-term-exposure studies are critical, since many of the cardiovascular events identified were correlated with PM exposure within the previous few hours (e.g., Peters et al. 2001). It should also be noted, however, that the cells might be able to adapt to the particles if exposures occurred over longer times; further research is needed to explore this issue. Although the in vitro concentrations that were used in the current study are likely to be greater than the plausible ambient concentrations of particles to which individuals might be exposed, our central conclusion is that the potential for inflammation varies with the type of metal oxide. We hypothesize that the differential response is related to the solubility of the metal oxides in the low pH environments that are seen in lysosomes. Any assessment of the health risks associated with exposure to metals may need to account for the composition of the metal fraction in aerosols.

The present study focused on the interactions of ultrafine particle with endothelial cells under static conditions. Endothelial cells in vivo are constantly exposed to flow, and there is mounting evidence that fluid mechanical forces play an important role in regulating endothelial

inflammation (Tedgui and Mallat 2001; Jiang et al. 2004; Ohno et al. 1995; Chappell et al. 1998). The presence of flow is also likely to alter the rate of delivery of nanoparticles to the endothelial cell surface and the time that particles interact with the cell surface. Therefore, future studies performed under conditions that simulate the flow in vivo promise to provide a more physiologically relevant understanding of endothelial cell inflammation induced by nanoparticles.

ACKNOWLEDGMENTS

The authors thank Grete Adamson, Patricia Kysar, and Xuqaio Feng for electron microscopy; Ryoji Shiraki for ICP–MS analyses; and Alexandra Navrotsky, John Neil, and Sergey Ushakov for the use of XRD and BET instruments and for related technical assistance. The majority of the cell studies were carried out by Dr. Andrea Gojova. The synthesis and characterization of particles was performed by Drs. Bing Guo and Heejung Jung, and also by Mr. Jutae Lee. Dr. Dosi Dosev assisted with the confocal microscopy. This research was also supported in part by grant DBI-010266 from the National Science Foundation, by grant 5P42ES04699 from the Superfund Basic Research Program, by grant P30-ES05705 from the National Institute of Environmental Health Sciences, and by grant HL55667 from the National Heart, Lung, and Blood Institute.

REFERENCES

Alfaro-Moreno E, Martinez L, Garcia-Cuellar C, Bonner JC, Murray JC, Rosas I, Rosales SP, Dsornio-Vargas AR. 2002. Biologic effects induced in vitro by PM10 from three different zones of Mexico City. Environ Health Perspect 110(7):715–720.

Brown DM, Stone V, Findlay P, MacNee W, Donaldson K. 2000. Increased inflammation and intracellular calcium caused by ultrafine carbon black is independent of transition metals or other soluble components. Occup Environ Med 57(10):685–691.

Carter WO, Narayanan PK, Robinson JP. 1994. Intracellular hydrogen peroxide and superoxide anion detection in endothelial cells. J Leukoc Biol 55(2):253–258.

Chappell DC, Varner SE, Nerem RM, Medford RM, Alexander RW. 1998. Oscillatory shear stress stimulates adhesion molecule expression in cultured human endothelium. Circ Res 82(5):532–539.

Dagher Z, Garcon G, Gosset P, Ledoux F, Surpateanu G, Courcot D, Aboukais A, Puskaric E, Shirali P. 2005. Pro-inflammatory effects of Dunkerque city air pollution particulate matter 2.5 in human epithelial lung cells (L132) in culture. J Appl Toxicol 25(2):166–175.

De Keulenaer GW, Chappell DC, Ishizaka N, Nerem RM, Alexander RW, Griendling KK. 1998. Oscillatory and steady laminar shear stress differentially affect human endothelial redox state: Role of a superoxide-producing NADH oxidase. Circ Res 82(10):1094–1101.

Donaldson K, Stone V, Seaton A, MacNee W. 2001. Ambient particle inhalation and the cardiovascular system: Potential mechanisms. Environ Health Perspect 109 Suppl 4:523–527.

Elder A, Gelein R, Finkelstein J, Phipps R, Frampton M, Utell M, Kittelson DB, Watts WF, Hopke P, Jeong CH, Kim E, Liu W, Zhao W, Zhuo L, Vincent R, Kumarathasan P, Oberdörster G. 2004. On-road exposure to highway aerosols. 2. Exposures of aged, compromised rats. Inhal Toxicol 16 Suppl 1:41–53.

Geiser M, Rothen-Rutishauser B, Kapp N, Schürch S, Kreyling W, Schulz H, Semmler M, Im Hof V, Heyder J, Gehr P. 2005. Ultrafine particles cross cellular membranes by nonphagocytic mechanisms in lungs and in cultured cells. Environ Health Perspect 113(11):1555–1560.

Guo B, Kennedy I. 2004. The speciation and morphology of chromium oxide nanoparticles in a diffusion flame. Aerosol Sci Technol 38(5):424–436.

Hinds W. 1999. Aerosol Technology: Properties, Behavior, and Measurement of Airborne Particles. 2nd ed. New York: John Wiley & Sons, Inc.

Huggins FE, Huffman GP, Robertson JD. 2000. Speciation of elements in NIST particulate matter SRMs 1648 and 1650. J Hazard Mater 74(1-2):1–23.

Jiang Z, Berceli SA, Pfahnl CL, Wu L, Goldman D, Tao M, Kagayama M, Matsukawa A, Ozaki CK. 2004. Wall shear modulation of cytokines in early vein grafts. J Vasc Surg 40(2):345–350.

Kreyling WG, Semmler M, Erbe F, Mayer P, Takenaka S, Schulz H, Oberdörster G, Ziesenis A. 2002. Translocation of ultrafine insoluble iridium particles from lung epithelium to extrapulmonary organs is size dependent but very low. J Toxicol Environ Health A 65(20):1513–1530.

Libby P. 2002. Inflammation in atherosclerosis. Nature 420(6917):868–874.

Liu SX, Athar M, Lippai I, Waldren C, Hei TK. 2001. Induction of oxyradicals by arsenic: Implication for mechanism of genotoxicity. Proc Natl Acad Sci USA 98:1643–1648.

Nel A, Xia T, Madler L, Li N. 2006. Toxic potential of materials at the nanolevel. Science 311(5761):622–627.

Nemmar A, Hoet PH, Dinsdale D, Vermylen J, Hoylaerts MF, Nemery B. 2003. Diesel exhaust particles in lung acutely enhance experimental peripheral thrombosis. Circulation 107(8):1202–1208.

Nemmar A, Hoet PH, Vanquickenborne B, Dinsdale D, Thomeer M, Hoylaerts MF, Vanbilloen H, Mortelmans L, Nemery B. 2002. Passage of inhaled particles into the blood circulation in humans. Circulation 105(4):411–414.

Noel NE, Ruthman JC. 1988. Elevated serum zinc levels in metal fume fever. Am J Emerg Med 6(6):609–610.

Ohno M, Cooke JP, Dzau VJ, Gibbons GH. 1995. Fluid shear stress induces endothelial transforming growth factor beta-1 transcription and production. Modulation by potassium channel blockade. J Clin Invest 95(3):1363–1369.

Ollinger K, Brunk UT. 1995. Cellular injury induced by oxidative stress is mediated through lysosomal damage. Free Radic Biol Med 19(5):565–574.

Panyam J, Labhasetwar V. 2003. Biodegradable nanoparticles for drug and gene delivery to cells and tissue. Adv Drug Deliv Rev 55(3):329–347.

Peters A, Dockery DW, Muller JE, Mittleman MA. 2001. Increased particulate air pollution and the triggering of myocardial infarction. Circulation 103(23):2810–2815.

Peters K, Unger RE, Kirkpatrick CJ, Gatti AM, Monari E. 2004. Effects of nano-scaled particles on endothelial cell function in vitro: Studies on viability, proliferation and inflammation. J Mater Sci Mater Med 15(4):321–325.

Pitsillides CM, Joe EK, Wei X, Anderson RR, Lin CP. 2003. Selective cell targeting with light-absorbing microparticles and nanoparticles. Biophys J 84(6):4023–4032.

Pope CA III, Burnett RT, Thurston GD, Thun MJ, Calle EE, Krewski D, Godleski JJ. 2004. Cardiovascular mortality and long-term exposure to particulate air pollution: Epidemiological evidence of general pathophysiological pathways of disease. Circulation 109(1):71–77.

Ross R. 1999. Atherosclerosis: An inflammatory disease. N Engl J Med 340(2):115–126.

Samet JM, Dominici F, Curriero FC, Coursac I, Zeger SL. 2000. Fine particulate air pollution and mortality in 20 U.S. cities, 1987–1994. N Engl J Med 343(24):1742–1749.

Schaumann F, Borm PJ, Herbrich A, Knoch J, Pitz M, Schins RP, Luettig B, Hohlfeld JM, Heinrich J, Krug N. 2004. Metal-rich ambient particles (particulate matter 2.5) cause airway inflammation in healthy subjects. Am J Respir Crit Care Med 170(8):898–903.

Schubert D, Dargusch R, Raitano J, Chan SW. 2006. Cerium and yttrium oxide nanoparticles are neuroprotective. Biochem Biophys Res Commun 342(1):86–91.

Spragg DD, Alford DR, Greferath R, Larsen CE, Lee KD, Gurtner GC, Cybulsky MI, Tosi PF, Nicolau C, Gimbrone MA Jr. 1997. Immunotargeting of liposomes to activated vascular endothelial cells: A strategy for site-selective delivery in the cardiovascular system. Proc Natl Acad Sci USA 94(16):8795–8800.

Tedgui A, Mallat Z. 2001. Anti-inflammatory mechanisms in the vascular wall. Circ Res 88(9):877–887.

Wagner M, Klein CL, van Kooten TG, Kirkpatrick CJ. 1998. Mechanisms of cell activation by heavy metal ions. J Biomed Mater Res 42(3):443–452.

Yamawaki H, Iwai N. 2006. Mechanisms underlying nanosized air-pollution-mediated progression of atherosclerosis: Carbon black causes cytotoxic injury/inflammation and inhibits cell growth in vascular endothelial cells. Circ J 70(1):129–140.

ABOUT THE AUTHORS

Ian M. Kennedy obtained his Ph.D. from Sydney University, Australia, in 1980. After a period as a research staff member at Princeton University and several years at the Aeronautical Research Laboratories in Australia, Kennedy joined the Department of Mechanical and Aeronautical Engineering at the University of California–Davis (UC Davis), in 1986, where he is currently a professor. At UC Davis he served as the vice-chair of the Department of Mechanical and Aeronautical Engineering for several years; he also served the College of Engineering as the associate dean for academic personnel and planning for four years. He developed a major combustion-generated aerosol and sensor research facility at UC Davis. The research there is focused on problems related to the formation of nanoparticles by gas-phase processes. A major thrust of Kennedy's work is the environmental impact of transportation systems, with a particular emphasis on the impact of aerosol nanoparticles on human health. He pursues this interest via extensive multidisciplinary collaborations with colleagues in the fields of environmental toxicology; land, air, and water resources; veterinary medicine; chemistry; and civil and environmental engineering.

Dennis Wilson obtained his D.V.M. from the University of Illinois in 1975 and his Ph.D. from UC Davis in 1983, where he is currently a professor in the Department of Pathology, Microbiology, and Immunology, School of Veterinary Medicine. He conducts clinical work on animal pathology and research into the health effects of air pollution.

Abdul I. Barakat is a professor of mechanical and aeronautical engineering at UC Davis and is on the faculty of the Biomedical Engineering, Biophysics, and Applied Mathematics Graduate Groups. Barakat obtained a B.S. in nuclear engineering from North Carolina State University and an M.S. in nuclear engineering from the Massachusetts Institute of Technology. He received a Ph.D. in chemical engineering from MIT in 1994, where his dissertation research focused on the role of fluid mechanical forces in regulating macromolecular transport within the arterial wall. He subsequently spent a year as a National Institutes of Health postdoctoral fellow at the University of Chicago before joining UC Davis in 1995 as an assistant professor.

OTHER PUBLICATIONS RESULTING FROM THIS RESEARCH

Gojova A, Guo B, Kota RS, Rutledge JC, Kennedy IM, Barakat AI. 2007. Induction of inflammation in vascular endothelial cells by metal oxide nanoparticles: Effect of particle composition. Environ Health Perspect 115(3):403–409.

ABBREVIATIONS AND OTHER TERMS

ANOVA	analysis of variance
BET	Brunauer-Emmett-Teller [method]
cDNA	complementary DNA
CeO_2	cerium oxide
CMD	count median diameter
CM-H_2DCFDA	5-[and-6]-chloromethyl-2′,7′-dichlorodihydrofluorescein diacetate, acetyl ester
CPC	condensation particle counter
DHE	dihydroethidium
ELISA	enzyme-linked immunosorbent assay
Eu:Y_2O_3	europium-doped Y_2O_3 particles
Fe_2O_3	iron oxide
$Fe(CO)_5$	iron pentacarbonyl
GAPDH	glyceraldehyde-3-phosphate dehydrogenase
GCLC	glutamate-cysteine ligase
GMD	geometric mean diameter
GSD	geometric standard deviation
HAECs	human aortic endothelial cells
HBSS	Hanks balanced salt solution
HMOX1	heme oxygenase 1
HNO_3	nitric acid
H_2O_2	hydrogen peroxide
HRP	horseradish peroxidase
HUVEC	human umbilical-vein endothelial cell
ICAM-1	intercellular adhesion molecule-1
ICP–MS	inductively coupled plasma–mass spectrometry
IL-8	interleukin-8
LSGS	low serum growth supplement
MCP-1	monocyte chemotactic protein-1
mRNA	messenger RNA
NADPH	nicotinamide adenine dinucleotide phosphate
NIST	National Institute of Standards and Technology
NOX4	NADPH oxidase 4
PBS	phosphate-buffered saline
PM	particulate matter
$PM_{2.5}$	particulate matter ≤ 2.5 μm in aerodynamic diameter
PM_{10}	particulate matter ≤ 10 μm in aerodynamic diameter
ROS	reactive oxygen species
RT–PCR	reverse transcriptase–polymerase chain reaction
SiO_2	silicon dioxide
SMPS	scanning mobility particle sizer
SRM	standard reference material
TEM	transmission electron microscopy
TiO_2	titanium dioxide
U.S. EPA	U.S. Environmental Protection Agency
XRD	x-ray diffraction
Y_2O_3	yttrium oxide
ZnO	zinc oxide

Research Report 136, *Uptake and Inflammatory Effects of Nanoparticles in a Human Vascular Endothelial Cell Line*, I.M. Kennedy et al.

INTRODUCTION

Ambient particulate matter (PM*) is a complex mixture of solid and liquid particles, ranging from approximately 0.005 to 100 μm in aerodynamic diameter, suspended in air. In addition to size, the chemical composition and other physical and biologic properties of PM vary spatially and temporally. This variability in PM characteristics derives from differences in the sources of pollution; these particles may be natural in origin—the result of geographic conditions, weather, or seasonal patterns—or generated by human activities such as driving vehicles and operating manufacturing or power plants.

Although the characteristics of PM differ from place to place, epidemiologic studies in diverse locations have reported associations between increases in levels of PM and short-term increases in cardiovascular morbidity and mortality. Long-term exposure to PM has also been associated with increased mortality from cardiopulmonary causes as well as from cancer (reviewed in U.S. Environmental Protection Agency [EPA] 2004). On the basis of these findings as well as the results of toxicologic studies, many governmental agencies have set regulatory standards or guidelines for levels of ambient PM. Particles ≤ 10 μm in aerodynamic diameter (PM_{10}) are of most concern because they are respirable in humans. To protect the general population and groups considered most vulnerable to adverse effects from PM in the United States, the EPA monitors PM_{10} levels and has promulgated National Ambient Air Quality Standards for particles ≤ 2.5 μm in aerodynamic diameter ($PM_{2.5}$, or fine particles). As discussed in the Scientific Background section below, some scientists believe that particles ≤ 100 nm in diameter may be particularly toxic: These particles are referred to as ultrafine (≤ 100 nm in all dimensions) or nanoparticles (with at least one dimension ≤ 100 nm; as defined by W. Kreyling, cited in Donaldson et al. 2005).

One of the key issues in assessing the health effects of PM is determining the chemical components and physical characteristics (size, charge, etc.) most responsible for toxicity. In addition, identifying the pathophysiological pathways by which these toxic components act is also critically important. Several studies, described in the Scientific Background section, have suggested that metals, and transition metals in particular, may be important toxic components of the PM mixture.

In November 2004, Dr. Ian Kennedy and colleagues at the University of California–Davis, submitted a preliminary application, "The Uptake of Ultrafine Particles by Vascular Endothelial Cells and Inflammation," in response to HEI's Request for Preliminary Applications RFPA 04-6. The investigators proposed to generate different ultrafine metal oxide particles (nanoparticles), evaluate their size, composition, and surface charge, and study their potential to induce inflammatory effects in human aortic endothelial cells (HAECs). The investigators also proposed to identify where inside the HAECs the particles would be found after co-culture with the cells. Because the responses of endothelial cells play a critical role in the development of atherosclerosis, the investigators proposed that the results of the studies would help to characterize the role that metal particles may play in the development or exacerbation of atherosclerosis.

The HEI Research Committee thought that Dr. Kennedy's hypothesis was sound, that his approach to detecting particles in cells was feasible, and that studying effects in endothelial cells was relevant. The Committee recommended to Dr. Kennedy that he submit a proposal for a pilot study to determine whether the proposed approaches would be successful. Consequently, Dr. Kennedy submitted a proposal for a one-year study; he and his team proposed to generate nanoparticles of the oxides of four metals—iron, zinc, yttrium, and cerium—and investigate their effects on HAECs in vitro. Kennedy and colleagues chose these metals because iron and zinc are abundant in urban and diesel exhaust PM (Huggins et al. 2000), iron and cerium are components of

* A list of abbreviations and other terms appears at the end of the Investigators' Report.

Dr. Kennedy's one-year study, "The Response of Endothelial Cells to Ultrafine Metal Oxide Particles," began in October 2005. Total expenditures were $142,622. The draft Investigators' Report from Ian Kennedy and colleagues was received for review in December 2006. A revised report, received in May 2007, was accepted for publication in June 2007. During the review process, the HEI Health Review Committee and the investigators had the opportunity to exchange comments and to clarify issues in both the Investigators' Report and in the Review Committee's Critique.

recently developed automobile technologies, and yttrium could be "tagged" with a fluorescent marker to identify the localization of particles taken up into HAECs. The Committee recommended the proposal for funding.

SCIENTIFIC BACKGROUND

THE TOXICITY OF ULTRAFINE PARTICLES

Ultrafine particles, emitted in high numbers by combustion engines, are the dominant contributors of particle numbers in $PM_{2.5}$. For example, a mass concentration of 10 µg particles/m^3 could contain only one fine particle of diameter 2.5 µm, but could contain more than 2 million ultrafine particles of diameter 0.02 µm (Oberdörster 1995). Smaller particles have a greater total surface area than larger particles of the same mass. Thus, they may present a larger surface area for interacting with airway tissue or for transporting toxic material associated with the particle surface into the airways.

Some scientists have hypothesized that ultrafine particles may be especially toxic (reviewed in Utell and Frampton 2000; Frampton 2001; Oberdörster 2001). Epidemiologic studies, however, have not resolved the issue of the comparative toxicity of ultrafine particles. Some studies have described associations between increases in adverse respiratory effects and exposure to ultrafine particles in children with asthma (Pekkanen et al. 1997; Peters et al. 1997). However, these studies found that exposure to ultrafine particles did not have a greater effect than exposure to fine particles. In addition, Wichmann and colleagues (2000) reported that mortality was associated with ultrafine particle concentrations in the city of Erfurt, Germany. However, the reported association was not greater than associations reported for mortality and other components of the PM mix. Peters and colleagues (2005), evaluating data on the induction of nonfatal myocardial infarction, did not find statistically significant associations with ultrafine particle concentrations at the time of the myocardial infarction or up to 5 days before it.

Toxicologic studies on the airways of rodents have compared the effects of exposure to high concentrations of particles of various sizes that have the same chemical composition (e.g., Oberdörster 1995). These studies have suggested that, based on mass, ultrafine particles are more potent than fine particles in inducing airway inflammatory responses. Initially these studies evaluated the effects of particles instilled intratracheally, but more recent studies have used inhalation, the more physiologically relevant route of exposure, to evaluate the effects of metals (Hahn et al. 2005) and carbon black particles (Gilmour et al. 2004). The inhalation studies have found a pattern similar to that of the intratracheal instillation studies, but they showed that composition also played a role.

THE TOXICITY OF METAL-CONTAINING PARTICLES

Many metals are found in PM in urban air, and adverse health effects—including inflammation and other cardiovascular responses—have been reported in studies of humans as well as nonhuman species exposed to metal-containing particles. Toxicologic studies with particles collected in the Utah Valley at times when a local steel plant was either open or closed suggested that transition metals had a key role in explaining prior epidemiologic findings—specifically, exposure to PM_{10} associated with decreased lung function and increased incidence of respiratory symptoms (Pope 1996). The magnitude of the inflammatory response induced in vivo or in vitro by the collected Utah Valley particles varied depending on the metal content of the particles (Dye et al. 2001; Ghio and Devlin 2001; Pagan et al. 2003).

Studies in rodents have documented cardiovascular and inflammatory effects of exposure to particles rich in transition metals—especially iron, nickel, and vanadium—emitted and collected from oil-fired and coal-fired electric power plants (residual oil fly ash and coal fly ash, respectively). Exposure to high levels of these particles in residual oil fly ash has been found to induce lung inflammation (Kadiiska et al. 1997), cardiac arrhythmias (Watkinson et al. 1998), and inflammatory cytokines in human bronchial epithelial cells (Carter et al. 1997). Exposure of rats via inhalation to high concentrations of nickel and vanadium affected cardiovascular responses and thermoregulation (Campen et al. 2001, 2002). In addition, Hahn and colleagues (2005) found that inhalation of either fine or ultrafine vanadium pentoxide particles resulted in inflammatory responses in rat airways.

Furthermore, the high temperatures used in welding generate a fume containing high concentrations of predominantly nano-sized metal particles, and studies suggest that welders develop adverse respiratory and systemic inflammatory and cardiovascular effects (reviewed in Antonini 2003; Donaldson et al. 2005). Welders of galvanized metals may also develop "metal fume fever," a flu-like condition accompanied by fever; the inhalation of zinc oxide particles is considered responsible (Kuschner et al. 1995).

OXIDATIVE STRESS

A voluminous literature exists on the generation of reactive oxygen species (ROS) and the development of oxidative

stress as plausible pathways to explain the induction of PM-mediated inflammatory responses. Under normal conditions, ROS—superoxide and oxygen-based free radicals, together with hydrogen peroxide—are cleared from cells by the action of enzymes such as superoxide dismutase and glutathione peroxidase or by other, nonenzymatic ROS scavengers. Oxidative stress is the result of an imbalance between the production of these oxidants and the local availability of antioxidants. Metals—including iron, zinc, and cerium—can initiate this state of oxidative stress, which may induce cell activation or cell damage (Smith et al. 2000; Tang et al. 2001; Aust et al. 2002; Manju et al. 2003; Nair et al. 2003). Intracellular signal-transduction pathways may be activated, resulting in the synthesis of inflammatory cytokines and chemokines that recruit inflammatory cells; production of these mediators by airway cells contributes to lung inflammation and injury (reviewed in Samet and Ghio 2007).

TRANSLOCATION OF INHALED PARTICLES OUT OF THE LUNG

Some studies have suggested that the toxicity of inhaled particles in the fine and ultrafine range may result from the particles' rapid translocation out of the lungs and into extrapulmonary tissues via the bloodstream (Takenaka et al. 2001; Kreyling et al. 2002; Nemmar et al. 2002; Kreyling et al. 2006; Peters et al. 2006). For example, Takenaka and colleagues (2001) detected particles of ultrafine silver in the blood of rats within a few hours after exposure via inhalation, and small amounts in several organs up to 7 days later. Kreyling and associates (2002) found deposition of ultrafine iridium particles in the liver, spleen, heart, and brain of rats 1 week after inhalation.

The investigators interpreted these findings to indicate that the inhaled particles crossed the pulmonary epithelial cell layer and were carried through the bloodstream to reach the tissues in which they were detected. Because the endothelium—a layer of specialized epithelial cells that lines the interior of blood vessels—serves as a barrier between tissues and the bloodstream, the passage of inhaled particles from lungs into the circulation and thence into tissue implies that particles have the opportunity to interact with the endothelial layer.

Inflammatory responses of the endothelium are considered critical in the development of atherosclerosis, the primary cause of many cardiovascular diseases (Libby 2002). How ultrafine particles interact with and alter endothelial cell function and how this interaction might be affected by particle composition has not been elucidated. Kennedy and colleagues sought to address these questions in the current study.

OVERVIEW OF AIMS, METHODS, AND RESULTS

STUDY AIMS

Kennedy and colleagues' primary objectives were to do the following:

1. Generate and physically characterize ultrafine cerium, iron, zinc, and yttrium oxide particles.
2. Compare the effects in HAECs of these particles on (a) markers of inflammation and (b) generation of ROS and oxidative stress.
3. Identify the location of nanoparticles inside endothelial cells.

CHANGES TO THE STUDY AIMS

Because the investigators encountered difficulties in generating nanoparticles of cerium oxide, few experiments were performed with this compound. In addition, the investigators originally proposed to measure a cassette of cytokines to assess the inflammatory response. In the study, however, they measured levels of only intercellular cell adhesion molecule-1 (ICAM-1), a cell-surface molecule whose expression is increased upon cell activation, and two chemokines: the neutrophil chemoattractant interleukin-8 (IL-8) and monocyte chemotactic protein-1 (MCP-1). They added measurements of RNA levels of three gene products involved in oxidative stress pathways: heme oxygenase 1 (HMOX1), glutamate-cysteine ligase catalytic subunit (GCLC), and NADPH oxidase 4 (NOX4).

STUDY DESIGN AND METHODS

PARTICLE SYNTHESIS AND CHARACTERIZATION

Kennedy and colleagues synthesized nanoparticles using a hydrogen/air diffusion flame seeded with vapors of different compositions: $Fe(CO)_5$ to make iron oxide, Fe_2O_3; tris(2,2,6,6-tetramethyl-3,5-heptanedionate)Y(III) to make yttrium oxide, Y_2O_3; and zinc metal vapor to make zinc oxide, ZnO. Because no suitable high-vapor-pressure precursor of cerium was available, the investigators used a soluble solid precursor, cerium acetate, and a spray flame burner to generate nanoparticles of cerium oxide, CeO_2 (Figure 1 in the Investigators' Report).

Kennedy and colleagues used several techniques to characterize the physical properties of the particles they generated: inductively coupled plasma–mass spectrometry (ICP–MS), to characterize the purity of the particles; X-ray diffraction (XRD), to measure the size of some of the

particles; transmission electron microscopy (TEM), also used to assess the localization of particles within HAECs; and a scanning mobility particle sizer (SMPS), to measure the size distributions of iron and cerium oxides in situ. The investigators also used the Brunauer-Emmett-Teller (BET) equation to estimate the particles' surface area; this approach uses the physical adsorption of a gas onto a solid surface to determine surface area (Hill 1996).

EXPOSURE OF ENDOTHELIAL CELLS TO METAL OXIDE NANOPARTICLES

The investigators used an HAEC line and grew cells to confluence through 5 to 8 passages in culture medium. They exposed the HAECs to nanoparticles at concentrations ranging from 0.001 to 50 μg/mL at 37°C. Cells were incubated with Fe_2O_3, Y_2O_3, or ZnO for 1 to 8 hours and with CeO_2 for 4 hours. Controls were not exposed to particles. Kennedy and colleagues used the trypan blue exclusion assay to assess the viability of cells exposed to particles after 4 hours. Cells exposed to zinc oxide particles were also evaluated after 24 hours in culture: cells incubated for 4 hours with zinc oxide were washed to remove extraneous particles and maintained in particle-free medium for a further 20 hours.

DETERMINATION OF INFLAMMATORY MARKERS

Using probes specific for ICAM-1, MCP-1, and IL-8, the investigators evaluated messenger RNA (mRNA) levels by reverse transcriptase–polymerase chain reaction (RT–PCR) in cells exposed for 4 hours to iron, yttrium, zinc, and cerium oxide particles. Further RT–PCR analysis was also performed on cells exposed to iron, yttrium, and zinc oxides for 1, 2, and 8 hours. The housekeeping gene glyceraldehyde-3-phosphate dehydrogenase (*GAPDH*) served as a control.

To measure ICAM-1 protein expressed on the surface of HAECs, the investigators used a rabbit polyclonal anti-ICAM-1 antibody in Western blot analysis; β-actin served as a control for ICAM-1 expression. Kennedy and colleagues used an enzyme-linked immunosorbent assay (ELISA) to measure levels of MCP-1 protein in the supernatant of HAECs. Cells exposed to cerium oxide were not analyzed for protein levels.

PARTICLE UPTAKE INTO CELLS AND INTRACELLULAR LOCALIZATION

Particle uptake

The investigators used ICP–MS to assess how much of the iron, yttrium, and zinc particles present in the culture medium became associated with HAECs over a 4-hour exposure period.

Intracellular localization

To identify the location of particles within cells, the investigators attempted to tag yttrium particles with fluorescent europium, which would fluoresce red at 612 nm. However, initial attempts to use europium-doped yttrium particles were not successful because the investigators found that subcellular structures such as mitochondria were more highly fluorescent than the particles. Thus, to determine the intracellular localization of zinc, yttrium, and iron oxide particles in HAECs after a 4-hour incubation, the investigators used TEM in fixed thin sections. The localization of iron oxide particles in HAECs after shorter incubation periods was also examined by this approach.

ROS GENERATION

The investigators used three fluorescence-based approaches to study the generation of ROS:

1. They grew HAECs on coverslips and loaded them with CM-H_2DCFDA (see Investigators' Report for further details), a compound that fluoresces in proportion to the level of intracellular oxidation. This approach was not successful.
2. The investigators also used dihydroethidium (DHE), a dye that fluoresces blue at 420 nm but when oxidized is converted to ethidium, which fluoresces red at 605 nm. Ethidium intercalates into the cell's DNA and stains the nucleus red.
3. The investigators also used a fluorescent antibody specific for the transcription factor Nrf2, which translocates to the nucleus as a consequence of intracellular ROS production.

OXIDATIVE STRESS

The investigators used probes specific for three genes that play a role in oxidative stress pathways: *HMOX1*, *GCLC*, and *NOX4*; *GAPDH* served as a control.

STATISTICAL ANALYSIS

The investigators analyzed data by one-way analysis of variance (ANOVA) and the Dunnett post-hoc test and showed data as means ± standard error.

RESULTS

The main results are summarized below and in Critique Table 1.

Critique Table 1. Main Results

Particle	Particle Characterization: Morphology and Size	Particle Characterization: Calculated Surface Area (mean ± SD) (m^2/g)	Intracellular Localization	Inflammatory Markers[a] (ICAM-1, MCP-1, IL-8): mRNA[b]	Inflammatory Markers[a] (ICAM-1, MCP-1, IL-8): Protein[b]	ROS and Oxidative Stress[a]: DHE[b]	ROS and Oxidative Stress[a]: Nrf2[b]	ROS and Oxidative Stress[a]: RT-PCR[c]
Fe_2O_3	Spherical Two size ranges Diameters 30–90 nm and < 5 nm	81 ± 1 (for the larger particles)	Cytoplasmic vesicles	–	–	–	–	–
Y_2O_3	Cubic, 2–60 nm Agglomerated	41 ± 1	Presumed degradation products in cytoplasmic vesicles	+	–	+	–	–
ZnO	Rod-shaped Length 100–200 nm Diameter 20–70 nm	20.8 ± 0.2	Few intracellular vesicles; high-density particles near cell membrane; some apparent discontinuities of membrane	+	+[d]	+	–	+ (HMOX1)
CeO_2	Spherical Diameter 28–38 nm	Approx. 19	NM	–	NM	NM	NM	NM

[a] + indicates statistically significant increase compared with controls ($P < 0.05$); – indicates not a statistically significant increase; NM indicates not measured.

[b] At particle concentration 50 µg/mL and with HAECs exposed for 4 hours.

[c] At particle concentration 10 µg/mL and with HAECs exposed for 4 hours.

[d] Measured only ICAM-1 and MCP-1.

CHARACTERIZATION OF PARTICLES

The investigators achieved their stated goals of generating nanoparticles of different composition and of characterizing some of the particles' physical characteristics. The nanoparticles generated varied in morphology (spherical, cubic, or rod-shaped), agglomeration, and size range (from spherical particles of iron oxide less than 5 nm in diameter to rod-shaped zinc oxide particles 100–200 nm long). Iron oxide particles were spherical and found in two size ranges: 30 to 90 nm in diameter and less than 5 nm in diameter (both nonagglomerated). The smaller particles, which the investigators suggest were generated by nucleation of gas-phase particles at the highest temperatures in the flame, accounted for approximately 28% of particle mass and 79% of particle surface area. Yttrium oxide particles were found as aggregates. The investigators reported that the particles did not contain metal contaminants.

BIOLOGIC EFFECTS OF PARTICLES ON HAECs

The metal oxides showed a range of effects on HAECs. Of the particles tested, zinc oxide was associated with the greatest number of effects. It increased protein and mRNA levels of markers of inflammation and one measure each of ROS generation and oxidative stress; zinc oxide particles also affected the adherence of HAECs to the substrate and may have resulted in death of the HAECs that became nonadherent. Yttrium oxide was associated with changes in a few end points: specifically, increases in mRNA of markers of inflammation and one measure of ROS. Iron oxide had no effect on any of the end points measured. Cerium oxide particles, evaluated in only a limited number of experiments (assessing the induction of markers of inflammation), had no effects.

PARTICLE INTERACTIONS WITH HAECs

Uptake

The amount of iron, yttrium, or zinc oxide particles associated with HAECs (1–100 pg/cell) measured after a 4-hour incubation period correlated directly with the concentration of particles (1–100 µg/mL) present in the culture medium (Figure 3 of the Investigators' Report).

Localization of particles

Only zinc, yttrium, and iron particles were tested. The appearance and localization of the three metal oxides

differed within the cell. Zinc oxide particles were seen in a few intracellular vesicles and near the cell membrane. At high magnification, the investigators reported that cells treated with zinc oxide showed some areas of discontinuity of the cell membrane (Figure 4, bottom-left image). Yttrium oxide particles were not as easily identified as iron oxide particles inside HAECs because the morphology of electron-dense material detected in HAECs differed from that of the originally generated particles (Figure 4, top-right image). This material was detected in cytoplasmic vesicles that the investigators characterized as swollen, the biologic significance of which is unclear. Iron oxide particles were identified in cytoplasmic vesicles (Figure 4, top-left image).

In additional experiments to examine the localization within HAECs after varying periods of co-culture with iron oxide particles, the investigators reported that after 30 minutes aggregates of particles accumulated near surface invaginations with ultrastructural characteristics of caveolae (Figure 8, top panel). After 4 hours, they reported that the accumulation of particles in intracytoplasmic vacuoles was accompanied by exocytosis of particles on the basilar surface (Figure 8, bottom panel).

HEI REVIEW COMMITTEE EVALUATION OF THE STUDY

Dr. Kennedy and colleagues conducted a one-year study that successfully generated nanoparticles of four different metal oxides and preliminarily investigated the biologic effects of the particles on an endothelial cell line in vitro. The Committee thought that the important contribution of this research was the generation and preliminary characterization of the metal oxide nanoparticles.

The Committee also agreed with the investigators' general conclusions about the biologic responses induced by the different particles: namely, that the effects induced by co-culture of HAECs with nanoparticles depended on the composition of the particles, with zinc oxide having the most effects and iron oxide none; cerium oxide, evaluated in only a few experiments, also had no effects. Zinc oxide particles also induced one effect not observed with the other particles: a loss of adherence of HAECs to the substrate. This effect of zinc oxide on the HAECs may also have been cytotoxic, although a specific test of cytotoxicity on nonadherent cells was not performed. How zinc oxide particles affected adherence or induced cytotoxicity was not studied. It is not possible to say whether the changes in ICAM-1, MCP-1, IL-8, or HMOX1 that the investigators measured in the remaining adherent cells were or were not related to the loss of adherence and viability.

The potency of zinc oxide particles in the current study on the induction of inflammatory and oxidative stress responses in HAECs is consistent with both in vitro and in vivo human and nonhuman studies (Fine et al. 1997; Tang et al. 2001; Kodavanti et al. 2008). The investigators report that the iron oxide particles they generated were taken up by HAECs and were detectable inside the cells; nonetheless, the iron oxide particles did not induce changes in inflammatory or oxidative stress end points. These findings are consistent with previous studies of the effects of iron particles (e.g., Guilianelli 1993; Lay et al. 1999; Smith et al. 2000; Aust et al. 2002; Stroh 2004), which indicate that different iron-containing compounds have different bioavailabilities and toxicities and that ferric oxide particles generally do not exert toxic effects. However, Kennedy, Pinkerton and colleagues have shown that inhalation of ultrafine ferric oxide particles induces some biologic responses in the airways of adult rats (Zhou et al. 2003; Pinkerton et al. 2008).

The composition-dependent differences among the particles in terms of in vitro biologic effects are consistent with the findings of Peters and colleagues (2007), who found differences in the biologic effects of cobalt and nickel on oxidative stress and inflammatory markers during co-culture with endothelial cells; both metal particles had cytotoxic effects. In addition, Yamawaki and Iwai (2006) reported that co-culture of vascular endothelial cells with carbon black induced some markers of inflammation and also induced cytotoxicity and the inhibition of cell growth.

The Committee thought the investigators' experiments defined some important differences in certain physical characteristics of the metal oxide particles. These included size, morphology, agglomeration, and calculated surface area. However, the Committee thought that these characteristics might also have played important roles in determining biologic responses and that the investigators had not thoroughly studied the roles of these differences among the particles generated. Thus, it was difficult to assess how these characteristics might have contributed to the differences in outcome. In addition, the investigators did not measure other features of the particles—such as surface charge or solubility—that might also have played important roles in contributing to the observed differences in biologic effects. Solubility may have been a particularly important characteristic to study. Kennedy and colleagues speculate that the differential solubility of the particles within acid compartments of the cell such as lysosomes, in which catabolism of many intracellular and extracellular components takes place, might explain the differences among particles in inducing inflammatory responses. The investigators did not perform any experiments to evaluate the solubility of particles at low pH, however.

The investigators calculated the surface areas of the nanoparticles they generated and concluded that the smaller the surface area of the particle, the greater the biologic effect on HAECs. This is not unreasonable since other studies have suggested that surface area is an important factor in determining particle effects (Oberdörster 1996; Stoeger et al. 2006; Monteiller et al. 2007; Donaldson et al. 2008). However, the Committee was uncertain whether the current study's findings supported this conclusion. In particular, the investigators' calculations indicated that the surface areas of cerium oxide and zinc oxide particles were very similar but that cerium oxide did not significantly affect markers of inflammation, whereas zinc oxide particles did. Moreover, the investigators found that approximately 25% of the iron oxide particles had a smaller diameter—and hence a smaller surface area per particle, but a larger surface area per unit mass—than all the other metal particles evaluated. Iron oxide particles, however, were inactive in the biologic assays. For these reasons the Committee found it difficult to conclude that the surface area of the nanoparticles generated correlated inversely with the inflammatory effects induced in HAECs.

The investigators also suggest that the different particles might have been taken up into different subcellular compartments or been associated with different organelles within the cell. However, the Committee thought these studies were difficult to interpret. The investigators had intended to use a europium-tagging technique with confocal microscopy to identify sites of particle localization within the HAECs, but because this was not successful they used electron microscopy, which was not as informative. The fate of yttrium oxide particles in these studies was particularly problematic because the particles detected within intracellular vesicles did not have the same morphology as the original particles. The investigators speculated that the particles they detected inside the cell were degradation products of the original particles. This may be correct, but how the particles may have been degraded within the HAECs was not clarified. It is also possible that the internalization of particles may have little or no relevance to the induction of intracellular effects: Particles may interact with a surface receptor—such as a Toll-like receptor—and activate inflammatory or oxidative stress pathways via signals transduced at the cell surface, rather than by internalization of the particles.

Extrapolating the current study's findings to in vivo human responses is challenging. The physiological relevance of the responses of endothelial cells in vitro to the concentrations of metal particles used in the current study is uncertain. As indicated in the Scientific Background section, exposure to high concentrations of inhaled metal particles is associated with adverse respiratory effects and systemic inflammatory and cardiovascular effects in welders and boilermakers (Kuschner et al. 1995; Wang et al. 2008; and reviewed in Antonini 2003; Donaldson et al. 2005). Sjögren and colleagues (2002) also reported that occupational exposure to welding fumes increased the risk of myocardial infarction. In addition, iron has been postulated to play a role in the induction of atherosclerosis (Yuan and Li 2008). Thus, characterization of the physical and chemical properties of well-defined metal oxide nanoparticles and the effects they induce in vivo and in vitro merits further study.

CONCLUSIONS

Kennedy and colleagues generated iron, zinc, yttrium, and cerium oxide nanoparticles and identified some of their important physical characteristics: size and shape, agglomeration, and calculated surface area. The investigators also performed preliminary studies to characterize effects of the different particles on inflammatory end points and the generation of ROS and oxidative stress in HAECs. The investigators found that the metal particles induced biologic responses in the endothelial cells and that the responses differed according to the composition of the particles: Zinc oxide particles showed the most effects, yttrium oxide fewer, and iron oxide none at all. Cerium oxide particles, evaluated in only a few experiments, had no effects.

The potency of zinc oxide particles in the current study on the induction of inflammatory and oxidative stress responses in HAECs is consistent with both in vitro and in vivo human and nonhuman studies. The investigators report that the iron oxide particles they generated were taken up by HAECs and were detectable inside the cells; nonetheless, the iron oxide particles did not induce changes in inflammatory or oxidative stress end points. These findings are consistent with previous studies of the effects of iron particles, which indicate that different iron-containing compounds have different bioavailabilities and toxicities and that ferric oxide particles generally do not exert toxic effects.

The Health Review Committee agreed with the investigators' general conclusions about the biologic responses induced by the different particles: namely, that the effects induced by co-culture of HAECs with nanoparticles depended on the composition of the particles. However, the Committee thought the differences in biologic responses of the particles may have resulted from differences not only in the chemical composition but also in their physical properties, such as those reported by the investigators, as

well as other, unexamined physical properties, such as solubility and surface charge. Thus, the Committee thought that the investigators had developed a potentially useful model system with HAECs, but that the study's results would have been strengthened if some of these other particle characteristics had been further explored.

Kennedy and colleagues also showed that the particles were taken up by HAECs, with some evidence that the particles may have localized to different compartments in the cells. This evidence was not clear-cut, however, and the Review Committee was not convinced that the reported biologic effects were related to differential localization of the particles within HAECs.

The investigators also proposed that biologic responses correlated inversely with the particle surface areas they calculated. Although particle surface area is likely to be one important factor in determining biologic effects, the HEI Review Committee was not convinced that the experiments the investigators had performed established a role for particle surface area in determining biologic outcomes.

Extrapolating the current study's findings to in vivo human responses is challenging. The physiological relevance of the responses of endothelial cells in vitro to the concentrations of metal particles used in the current study is uncertain. However, occupational exposure to high concentrations of inhaled metal particles has been associated with adverse respiratory and systemic inflammatory and cardiovascular effects. Thus, characterizing the physical and chemical properties of well-defined metal oxide nanoparticles and the effects they induce in vivo and in vitro merits further study.

ACKNOWLEDGMENTS

The Health Review Committee thanks the ad hoc reviewers for their help in evaluating the scientific merit of the Investigators' Report. The Committee is also grateful to Dr. Annemoon van Erp for her oversight of the study, to Elaine Nitta and Dr. Geoffrey Sunshine for their assistance in preparing its Critique, to Leah Shriro for science editing of this Report and its Critique, to Asterisk Typographics, Barre, Vermont, for composition, and to Virgi Hepner, Dr. Bernard Jacobson, Ruth E. Shaw, Flannery Carey McDermott, and Hope Green for their roles in preparing this Research Report for publication.

REFERENCES

Antonini, JM 2003. Health effects of welding. Crit Rev Toxicol 33(1):61–103.

Aust AE, Ball JC, Hu AA, Lighty JS, Smith KR, Straccia AM, Veranth JM, Young WC. 2002. Particle characteristics responsible for effects on human lung epithelial cells. Res Rep Health Effect Inst 110:1–65.

Campen MJ, Nolan JP, Schladweiler MC, Kodavanti UP, Costa DL, Watkinson WP. 2002. Cardiac and thermoregulatory effects of instilled particulate matter-associated transition metals in healthy and cardiopulmonary-compromised rats. J Toxicol Environ Health A 65:1615–1631.

Campen MJ, Nolan JP, Schladweiler MC, Kodavanti UP, Evansky PA, Costa DL, Watkinson WP. 2001. Cardiovascular and thermoregulatory effects of inhaled PM-associated transition metals: A potential interaction between nickel and vanadium sulfate. Toxicol Sci 64:243–252.

Carter JD, Ghio AJ, Samet JM, Devlin RB. 1997. Cytokine production by human airway epithelial cells after exposure to an air pollution particle is metal-dependent. Toxicol Appl Pharmacol 146:180–188.

Donaldson K, Borm PJ, Oberdörster G, Pinkerton KE, Stone V, Tran CL. 2008. Concordance between in vitro and in vivo dosimetry in the proinflammatory effects of low-toxicity, low-solubility particles: the key role of the proximal alveolar region. Inhal Toxicol 20:53–62.

Donaldson K, Tran L, Jimenez LA, Duffin R, Newby DE, Mills N, MacNee W, Stone V. 2005. Combustion-derived nanoparticles: A review of their toxicology following inhalation exposure. Part Fibre Toxicol 2(10):10.

Dye JA, Lehmann JR, McGee JK, Winslett DW, Ledbetter AD, Everitt JL, Ghio AJ, Costa DL. 2001. Acute pulmonary toxicity of particulate matter filter extracts in rats: Coherence with epidemiologic studies in Utah Valley residents. Environ Health Perspect 109(Suppl 3):395–403.

Fine JM, Gordon T, Chen LC, Kinney P, Falcone G, Beckett WS. 1997. Metal fume fever: characterization of clinical and plasma IL-6 responses in controlled human exposures to zinc oxide fume at and below the threshold limit value. J Occup Environ Med 39:722–726.

Frampton MW. 2001. Systemic and cardiovascular effects of airway injury and inflammation: Ultrafine particle exposure in humans. Environ Health Perspect 109:529–532.

Ghio AJ, Devlin RB. 2001. Inflammatory lung injury after bronchial installation of air pollution particles. Am J Respir Crit Care Med 164:704–708.

Gilmour PS, Ziesenis A, Morrison ER, Vickers MA, Drost EM, Ford I, Karg E, Mossa C, Schroeppel A, Ferron GA, Heyder J, Greaves M, MacNee W, Donaldson K. 2004.

Pulmonary and systemic effects of short-term inhalation exposure to ultrafine carbon black particles. Toxicol Appl Pharmacol 195:35–44.

Guilianelli C, Baeza-Squiban A, Boisvieux-Ulrich E, Houcine O, Zalma R, Guennou C, Pezerat H, Marano F. 1993. Effect of mineral particles containing iron on primary cultures of rabbit tracheal epithelial cells: Possible implication of oxidative stress. Environ Health Perspect 101:436–442.

Hahn FF, Barr EB, Ménache MG, Seagrave JC. 2005. Particle size and composition related to adverse health effects in aged, sensitive rats. Research Report 129. Health Effects Institute, Boston, MA.

Hill TL. 1996. Adsorption from a one-dimensional lattice gas and the Brunauer-Emmett-Teller equation. Proc Natl Acad Sci 93:14328–14332.

Huggins FE, Huffman GP, Robertson JD 2000. Speciation of elements in NIST particulate matter SRMs 1648 and 1650. J Hazardous Materials 74:1–23.

Kadiiska MB, Mason RP, Dreher KL, Costa DL, Ghio AF. 1997. In vivo evidence of free radical formation in the rat lung after exposure to an emission source air pollution particle. Chem Res Toxicol 10:1104–1108.

Kodavanti UP, Schladweiler MC, Gilmour PS, Wallenborn JG, Mandavilli BS, Ledbetter AD, Christiani DC, Runge MS, Karoly ED, Costa DL, Peddada S, Jaskot R, Richards JH, Thomas R, Madamanchi NR, Nyska A. 2008. The role of particulate matter-associated zinc in cardiac injury in rats. Environ Health Perspect 116:13–20.

Kreyling WG, Semmler M, Erbe F, Mayer P, Takenaka S, Schulz H, Oberdörster G, Ziesenis A. 2002. Translocation of ultrafine insoluble iridium particles from lung epithelium to extrapulmonary organs is size dependent but very low. J Toxicol Environ Health A 65(20):1513–1530.

Kuschner WG, D'Alessandro A, Wintermeyer SF, Wong H, Boushey HA, Blanc PD. 1995. Pulmonary responses to purified zinc oxide fume. J Investig Med 43(4):371–378.

Lay JC, Bennett WD, Ghio AJ, Bromberg PA, Costa DL, Kim CS, Koren HS, Devlin RB. 1999. Cellular and biochemical response of the human lung after intrapulmonary instillation of ferric oxide particles. Am J Respir Cell Mol Biol 20:631–642.

Libby P. 2002. Inflammation in atherosclerosis. Nature 420 (6917):868–874.

Manju L, Remani K, Nair RR. 2003. Negative inotropic response to cerium in ventricular papillary muscle is mediated by reactive oxygen species. Biol Trace Elem Res 96 (1–3):203–208.

Monteiller C, Tran L, MacNee W, Faux S, Jones A, Miller B, Donaldson K. 2007. The pro-inflammatory effects of low-toxicity low-solubility particles, nanoparticles and fine particles, on epithelial cells in vitro: The role of surface area. Occup Environ Med 64:609–615.

Nair RR, Preeta R, Smitha G, Adiga I. 2003. Variation in mitogenic response of cardiac and pulmonary fibroblasts to cerium. Biol Trace Elem Res 94(3):237–246.

Nemmar A, Hoet PH, Vanquickenborne B, Dinsdale D, Thomeer M, Hoylaerts MF, Vanbilloen H, Mortelmans L, Nemary B. 2002. Passage of inhaled particles into the blood circulation in humans. Circulation 105:411–414.

Oberdörster G. 1995. Lung particle overload: Implications for occupational exposures to particles. Regul Toxicol Pharmacol 21:123–135.

Oberdörster G. 1996. Significance of particle parameters in the evaluation of exposure-dose-response relationships of inhaled particles. Inhal Toxicol 8 Suppl:73–89.

Oberdörster G. 2001. Pulmonary effects of inhaled ultrafine particles. Int Arch Occup Environ Health 74:1–8.

Pagan I, Costa DL, McGee JK, Richards JH, Dye JA. 2003. Metals mimic airway epithelial injury induced by in vitro exposure to Utah Valley ambient particulate matter extracts. J Toxicol Environ Health A 66:1087–1112.

Pekkanen J, Timonen KL, Ruuskanen J, Reponen A, Mirme A. 1997. Effects of ultrafine and fine particles in urban air on peak expiratory flow among children with asthmatic symptoms. Environ Res 74:24–33.

Peters A, Wichmann HE, Tuch T, Heinrich J, Heyder J. 1997. Respiratory effects are associated with the number of ultrafine particles. Am J Respir Crit Care Med 155:1376–1383.

Peters K, Unger RE, Gatti AM, Sabbioni E, Tsaryk R, Kirkpatrick CJ. 2007. Metallic nanoparticles exhibit paradoxical effects on oxidative stress and pro-inflammatory response in endothelial cells in vitro. Int J Immunopathol Pharmacol 20:685–695.

Pinkerton KE, Zhou Y, Zhong C, Smith KR, Teague SV, Kennedy IM, Ménache MG. 2008. Mechanisms of Particulate Matter Toxicity in Neonatal and Young Adult Rat Lungs. Research Report 135. Health Effects Institute, Boston, MA.

Pope CA III. 1996. Particulate pollution and health: A review of the Utah valley experience. J Expo Anal Environ Epidemiol 6:23–34.

Samet JM, Ghio AJ. 2007. Particle-associated metals and oxidative stress in signaling. In: Particle Toxicology. (Donaldson K and Borm P, eds.) pp 161–181. CRC Press.

Schaumann F, Borm PJ, Herbrich A, Knoch J, Pitz M, Schains RP, Luettig B, Hohlfeld JM, Heinbrich J, Krug N. 2004. Metal-rich ambient particles (particulate matter 2.5) cause airway inflammation in health subjects. Am J Respir Crit Care Med 170:898–903.

Sjögren B, Fossum T, Lindh T, and Weiner J. 2002. Welding and ischemic heart disease. Int J Occup Environ Health 8(4):309–311.

Smith KR, Veranth JM, Hu AA, Lighty JS, Aust AE. 2000. Interleukin-8 levels in human lung epithelial cells are increased in response to coal fly ash and vary with bioavailability of iron, as a function of particle size and source of coal. Chem Res Toxicol 13:118–125.

Stoeger T, Reinhard C, Takenaka S, Schroeppel A, Karg E, Ritter B, Heyder J, Schulz H. 2006. Instillation of six different ultrafine carbon particles indicates a surface area threshold dose for acute lung inflammation in mice. Environ Health Perspect 114:328–333.

Stroh A, Zimmer C, Gutzeit C, Jakstadt M, Marschinke F, Jung T, Pilgrimm H, Grune T. 2004. Iron oxide particles for molecular magnetic resonance imaging cause transient oxidative stress in rat macrophages. Free Radic Biol Med 36:976–984.

Takenaka S, Karg E, Roth C, Schulz H, Ziesenis A, Heinzmann U, Schramel P, Heyder J. 2001. Pulmonary and systemic distribution of inhaled ultrafine silver particles in rats. Environ Health Perspect 109 Suppl 4:547–551.

Tang ZL, Wasserloos K, St Croix CM, Pitt BR. 2001. Role of zinc in pulmonary endothelial cell response to oxidative stress. Am J Physiol Lung Cell Mol Physiol 281(1):L243–L249.

U.S. Environmental Protection Agency. 2004. Air Quality Criteria for Particulate Matter. EPA/600/P-99/002aF. National Center for Environmental Assessment, Office of Research and Development, U.S. Environmental Protection Agency, Research Triangle Park, NC.

Utell MJ, Frampton MW. 2000. Acute health effects of ambient air pollution: The ultrafine particle hypothesis. J Aerosol Med 13:355–359.

Wang Z, Neuberg D, Su L, Kim JY, Chen JC, Christiani DC. 2008. Prospective study of metal fume-induced responses of global gene expression profiling in whole blood. Inhal Toxicol. 20:1233–1244.

Watkinson WP, Campen MJ, Costa DL. 1998. Cardiac arrhythmia induction after exposure to residual oil fly ash particles in a rodent model of pulmonary hypertension. Toxicol Sci 41:209–216.

Yamawaki H, Iwai N. 2006. Mechanisms underlying nanosized air-pollution-mediated progression of atherosclerosis: carbon black causes cytotoxic injury/inflammation and inhibits cell growth in vascular endothelial cells. Circ J 70:129–140.

Yuan XM, Li W. 2008. Iron involvement in multiple signaling pathways of atherosclerosis: a revisited hypothesis. Curr Med Chem 15:2157–2172.

Zhou YM, Zhong CY, Kennedy IM, Pinkerton KE. 2003. Pulmonary responses of acute exposure to ultrafine iron particles in healthy adult rats. Environ Toxicol 18:227–235.

RELATED HEI PUBLICATIONS: PARTICULATE MATTER AND DIESEL EXHAUST

Number	Title	Principal Investigator	Date*
Research Reports			
134	Black-Pigmented Material in Airway Macrophages from Healthy Children: Association with Lung Function and Modeled PM_{10}	J. Grigg	2008
131	Characterization of Particulate and Gas Exposures of Sensitive Subpopulations Living in Baltimore and Boston	P. Koutrakis	2005
129	Particle Size and Composition Related to Adverse Health Effects in Aged, Sensitive Rats	F.F. Hahn	2005
128	Neurogenic Responses in Rat Lungs After Nose-Only Exposure to Diesel Exhaust	M.L. Witten	2005
127	Personal, Indoor, and Outdoor Exposures to $PM_{2.5}$ and Its Components for Groups of Cardiovascular Patients in Amsterdam and Helsinki	B. Brunekreef	2005
126	Effects of Exposure to Ultrafine Carbon Particles in Healthy Subjects and Subjects with Asthma	M.W. Frampton	2004
124	Particulate Air Pollution and Nonfatal Cardiac Events		2005
	Part I. Air Pollution, Personal Activities, and Onset of Myocardial Infarction in a Case–Crossover Study	A. Peters	
	Part II. Association of Air Pollution with Confirmed Arrhythmias Recorded by Implanted Defibrillators	D. Dockery	
120	Effects of Concentrated Ambient Particles on Normal and Hypersecretory Airways in Rats	J.R. Harkema	2004
118	Controlled Exposures of Healthy and Asthmatic Volunteers to Concentrated Ambient Particles in Metropolitan Los Angeles	H. Gong Jr.	2003
112	Health Effects of Acute Exposure to Air Pollution	S.T. Holgate	2003
	Part I. Healthy and Asthmatic Subjects Exposed to Diesel Exhaust		
	Part II. Healthy Subjects Exposed to Concentrated Ambient Particles		
110	Particle Characteristics Responsible for Effects on Human Lung Epithelial Cells	A.E. Aust	2002
104	Inhalation Toxicology of Urban Ambient Particulate Matter: Acute Cardiovascular Effects in Rats	R. Vincent	2001
99	A Case–Crossover Analysis of Fine Particulate Matter Air Pollution and Out-of-Hospital Sudden Cardiac Arrest	H. Checkoway	2000
98	Daily Mortality and Fine and Ultrafine Particles in Erfurt, Germany *Part I.* Role of Particle Number and Particle Mass	H-E. Wichmann	2000

Continued

** Reports published since 1995.*
Copies of these reports can be obtained from the Health Effects Institute and many are available at www.healtheffects.org.

RELATED HEI PUBLICATIONS: PARTICULATE MATTER AND DIESEL EXHAUST

Number	Title	Principal Investigator	Date*
97	Identifying Subgroups of the General Population That May Be Susceptible to Short-Term Increases in Particulate Air Pollution: A Time-Series Study in Montreal, Quebec	M.S. Goldberg	2000
96	Acute Pulmonary Effects of Ultrafine Particles in Rats and Mice	G. Oberdörster	2000
95	Association of Particulate Matter Components with Daily Mortality and Morbidity in Urban Populations	M. Lippmann	2000
91	Mechanisms of Morbidity and Mortality from Exposure to Ambient Air Particles	J.J. Godleski	2000
Special Reports			
	Revised Analyses of Time-Series Studies of Air Pollution and Health		2003
	Research Directions to Improve Estimates of Human Exposure and Risk from Diesel Exhaust		2002
	Reanalysis of the Harvard Six Cities Study and the American Cancer Society Study of Particulate Air Pollution and Mortality: A Special Report of the Institute's Particle Epidemiology Reanalysis Project		2000
	Diesel Emissions and Lung Cancer: Epidemiology and Quantitative Risk Assessment		1999
	Particulate Air Pollution and Daily Mortality: The Phase I Report of the Particle Epidemiology Evaluation Project		
	Phase I.A. Replication and Validation of Selected Studies		1995
	Phase I.B. Analyses of the Effects of Weather and Multiple Air Pollutants		1997
	Diesel Exhaust: A Critical Analysis of Emissions, Exposure and Health Effects		1995
HEI Communications			
8	The Health Effects of Fine Particles: Key Questions and the 2003 Review (Report of the Joint Meeting of the EC and HEI)		1999
HEI Research Program Summaries			
	Research on Particulate Matter		1999
HEI Perspectives			
	Understanding the Health Effects of Components of the Particulate Matter Mix: Progress and Next Steps		2002
	Airborne Particles and Health: HEI Epidemiologic Evidence		2001

** Reports published since 1995.*
Copies of these reports can be obtained from the Health Effects Institute and many are available at www.healtheffects.org.

HEI BOARD, COMMITTEES, and STAFF

Board of Directors

Richard F. Celeste, Chair *President, Colorado College*

Enriqueta Bond *Past President, Burroughs Wellcome Fund*

Purnell W. Choppin *President Emeritus, Howard Hughes Medical Institute*

Jared L. Cohon *President, Carnegie Mellon University*

Stephen Corman *President, Corman Enterprises*

Gowher Rizvi *Vice Provost, University of Virginia*

Linda Rosenstock *Dean, School of Public Health, University of California–Los Angeles*

Archibald Cox, Founding Chair *1980–2001*

Donald Kennedy, Vice Chair Emeritus *Editor-in-Chief Emeritus,* Science; *President Emeritus and Bing Professor of Biological Sciences, Stanford University*

Health Research Committee

Mark J. Utell, Chair *Professor of Medicine and Environmental Medicine, University of Rochester Medical Center*

Kenneth L. Demerjian *Ray Falconer Endowed Chair and Director, Atmospheric Sciences Research Center and Department of Earth and Atmospheric Science, University at Albany, State University of New York*

Joe G.N. Garcia *Lowell T. Coggeshall Professor of Medicine and Chair, Department of Medicine, University of Chicago*

Uwe Heinrich *Executive Director, Fraunhofer Institute of Toxicology and Experimental Medicine, Hanover, Germany*

Grace LeMasters *Professor of Epidemiology and Environmental Health, University of Cincinnati College of Medicine*

Sylvia Richardson *Professor of Biostatistics, Department of Epidemiology and Public Health, Imperial College School of Medicine, London, United Kingdom*

Howard E. Rockette *Professor and Chair, Department of Biostatistics, Graduate School of Public Health, University of Pittsburgh*

James A. Swenberg *Kenan Distinguished Professor of Environmental Sciences, Department of Environmental Sciences and Engineering, University of North Carolina–Chapel Hill*

Ira B. Tager *Professor of Epidemiology, School of Public Health, University of California–Berkeley*

HEI BOARD, COMMITTEES, and STAFF

Health Review Committee

Homer A. Boushey, Chair *Professor of Medicine, Department of Medicine, University of California–San Francisco*

Ben Armstrong *Reader in Epidemiological Statistics, Department of Public Health and Policy, London School of Hygiene and Tropical Medicine, United Kingdom*

Michael Brauer *Professor, School of Environmental Health, University of British Columbia, Canada*

Bert Brunekreef *Professor of Environmental Epidemiology, Institute of Risk Assessment Sciences, University of Utrecht, the Netherlands*

Alan Buckpitt *Professor of Toxicology, Department of Molecular Biosciences, School of Veterinary Medicine, University of California–Davis*

John R. Hoidal *A.D. Renzetti Jr. Presidential Professor and Chair, Department of Medicine, University of Utah Health Sciences Center*

Stephanie London *Senior Investigator, Epidemiology Branch, National Institute of Environmental Health Sciences*

William N. Rom *Sol and Judith Bergstein Professor of Medicine and Environmental Medicine and Director of Pulmonary and Critical Care Medicine, New York University Medical Center*

Armistead Russell *Georgia Power Distinguished Professor of Environmental Engineering, School of Civil and Environmental Engineering, Georgia Institute of Technology*

Officers and Staff

Daniel S. Greenbaum *President*
Robert M. O'Keefe *Vice President*
Rashid Shaikh *Director of Science*
Barbara Gale *Director of Publications*
Jacqueline C. Rutledge *Director of Finance and Administration*
Helen I. Dooley *Corporate Secretary*

Kate Adams *Staff Scientist*
Marian Berkowitz *Research Associate*
Aaron J. Cohen *Principal Scientist*
Maria G. Costantini *Principal Scientist*
Philip J. DeMarco *Compliance Manager*
Terésa Fasulo *Science Administration Manager*
Hope Green *Editorial Assistant (part time)*
L.Virgi Hepner *Senior Science Editor*
Debra A. Kaden *Principal Scientist*
Anny Luu *Administrative Assistant*
Francine Marmenout *Senior Executive Assistant*
Flannery Carey McDermott *Editorial Assistant*
Teresina McGuire *Accounting Assistant*
Sumi Mehta *Senior Scientist*
Nicholas Moustakas *Policy Associate*
Tiffany North *Research Associate*
Kelly Pitts *Research Assistant*
Hilary Selby Polk *Science Editor*
Robert A. Shavers *Operations Manager*
Geoffrey H. Sunshine *Senior Scientist*
Annemoon M.M. van Erp *Senior Scientist*

HEALTH
EFFECTS
INSTITUTE

101 Federal Street, Suite 500
Boston, MA 02110, USA
+1-617-488-2300
www.healtheffects.org

RESEARCH
REPORT

Number 136
January 2009